



3 4456 0320396 8

ORNL/TM-11468

# ornl

**OAK RIDGE  
NATIONAL  
LABORATORY**

**MARTIN MARIETTA**

## Periodic Trajectories for Two-Dimensional Nonintegrable Hamiltonians

(A report based on a talk presented at the  
ORNL Chaos Workshop, January 10-11, 1990)

K. T. R. Davies

OAK RIDGE NATIONAL LABORATORY  
CENTRAL RESEARCH LIBRARY  
CIRCULATION SECTION  
4309E BLDG 175  
**LIBRARY LOAN COPY**  
DO NOT TRANSFER TO ANOTHER PERSON  
If you wish someone else to use this  
report, send in name with report and  
the library will arrange a loan.

OPERATED BY  
MARTIN MARIETTA ENERGY SYSTEMS, INC.  
FOR THE UNITED STATES  
DEPARTMENT OF ENERGY

This report has been reproduced directly from the best available copy.

Available to DOE and DOD contractors from the Office of Scientific and Technical Information, P.O. Box 62, Oak Ridge, TN 37831; prices available from (615) 578-8401, FTS 626-8401.

Available to the public from the National Technical Information Service, U.S. Department of Commerce, 5285 Port Royal Rd., Springfield, VA 22161.

NTIS price codes—Printed Copy: A05 Microfiche A01

This report was prepared as an account of work sponsored by an agency of the United States Government. Neither the United States Government nor any agency thereof, nor any of their employees, makes any warranty, express or implied, or assumes any legal liability or responsibility for the accuracy, completeness, or usefulness of any information, apparatus, product, or process disclosed, or represents that its use would not infringe privately owned rights. Reference herein to any specific commercial product, process, or service by trade name, trademark, manufacturer, or otherwise, does not necessarily constitute or imply its endorsement, recommendation, or favoring by the United States Government or any agency thereof. The views and opinions of authors expressed herein do not necessarily state or reflect those of the United States Government or any agency thereof.

Physics Division

PERIODIC TRAJECTORIES FOR TWO-DIMENSIONAL NONINTEGRABLE  
HAMILTONIANS

(a report based on a talk presented at the ORNL Chaos Workshop,  
January 10-11, 1990)

K.T.R. Davies

Date published - February 1990

Prepared for

U.S. Department of Energy Division of Nuclear Physics

Prepared by the  
OAK RIDGE NATIONAL LABORATORY  
Oak Ridge, Tennessee 37831-2008  
operated by  
MARTIN MARIETTA ENERGY SYSTEMS, INC.  
FOR THE  
U.S. DEPARTMENT OF ENERGY  
under contract DE-AC05-84OR21400





## CONTENTS

I. Introduction	I-1
II. Theory	II-1
III. Results	III-1
A. Topology of the E- $\tau$ Plots	III-1
B. Branching Behavior	III-8
IV. Nonperiodic Trajectories	IV-1
V. Calculation of Invariant Tori	V-1
VI. Conclusions	VI-1
VII. References	VII-1
VIII. Figures	VIII-1



## I. INTRODUCTION

I want to report on some calculations of classical periodic trajectories in a two-dimensional nonintegrable potential. This work was done in collaboration with M. Baranger, C. P. Malta, M.A.M. de Aguiar, J. M. Mahoney, M. Kargarlis, W. Saphir, and T. Huston.<sup>1-7</sup> After a brief introduction, I will present some details of the theory. The main part of this report will be devoted to showing pictures of the various families of trajectories and to discussing the topology (in  $E-\tau$  space) and branching behavior of these families. Then I will demonstrate the connection between periodic trajectories and "nearby" nonperiodic trajectories, which nicely illustrates the relationship of this work to chaos. Finally, I will discuss very briefly how periodic trajectories can be used to calculate tori.<sup>12</sup>

The initial motivation for this work really came from our interest in nuclear collective motion and quantization using classical trajectories.<sup>1</sup> You might ask the question: why should one quantize a classical approximation rather than simply solve the Schrödinger equation? The answer is that in a complicated many-body problem one often obtains approximate solutions in the form of time-dependent wave packets, following classical trajectories. This description applies to the time-dependent Hartree-Fock (TDHF) studies, which have been on active research effort here at ORNL for many years.<sup>11</sup>

At this point, I digress a bit to discuss some TDHF results which early on stimulated my interest in periodic motion and chaotic behavior

in nuclear physics. About 1985 Sait Umar, Mike Strayer, and collaborators<sup>11</sup> completed some very beautiful studies in TDHF which nicely demonstrated nonlinear behavior. Figure 1 from their work shows isoscalar density ( $\rho_n + \rho_p$ ) contour plots for the time evolution of the collision of two  $^{12}\text{C}$  ions, each of which initially is in a different configuration. The motion is rapid, giving rise to different multipole moments of the shape. In Fig. 2, they plot the main multipole moments of this  $^{12}\text{C} + ^{12}\text{C} \rightarrow ^{24}\text{Mg}$  system. The upper curve gives the isovector dipole moment as a function of time, while the middle and lower curves display the isoscalar quadrupole and octupole moments, respectively. Going from top to bottom, the curves increasingly become less chaotic. Note that the quadrupole moment undergoes damping, while the octupole moment has a very pronounced quasiperiodicity. In Fig. 3, they display Poincaré sections of the isoscalar quadrupole and octupole modes for this system. Here they plot moment velocities as a function of moments. The octupole motion is focused into a band of trajectories, while the quadrupole motion is clearly much more chaotic. (However, we remark that the quadrupole and octupole motions are strongly coupled to each other.) All of this is very suggestive of the kinds of quasiperiodic and chaotic results seen in many other fields. Again because of the classical-like nature of the TDHF approximation, there is a strong motivation for extending the classical studies of periodic motion to TDHF; this is a project we plan to work on. I shall now return to the main theme: the study of classical periodic trajectories.

However, there is one remaining question, namely why should one quantize using classical periodic trajectories?<sup>1</sup> The answer is given to

us in a famous quotation<sup>1</sup> by Henri Poincaré, who said, "What renders these periodic solutions so precious to us is that they are, so to speak, the only breach through which we might try to penetrate into a stronghold hitherto reputed unassailable." That is, periodic trajectories carry all possible information about the dynamics, and they are easier to work with than the nonperiodic trajectories since time integrals need only be done over one period, rather than from  $-\infty$  to  $+\infty$ . (One can always refine the answers by examining longer periods.)

There is another quote about chaos that I am fond of. In his book "Computational Physics", Steve Koonin<sup>8</sup> says that for certain nonlinear calculations "...computer results defy our intuition (and thereby reshape it) and numerical work is essential for a proper understanding." For much of the work I am about to describe, I found that time and time again my intuition was incorrect regarding what to expect, and the computer results kept pointing us in new, exciting directions. Now, of course, in retrospect many of the phenomena that we discovered seem rather obvious, but I will try to emphasize those features which were initially unexpected and which I suspect will not be so obvious to most of you.



## II. THEORY

First, a few words about the equations of motion. We solve Hamilton's equations in a two-dimensional space<sup>1-7</sup>

$$\ddot{x} + \frac{\partial V(x,y)}{\partial x} = 0$$

$$\ddot{y} + \frac{\partial V(x,y)}{\partial y} = 0,$$

where

$$H = \frac{1}{2} (p_x^2 + p_y^2) + V(x,y).$$

These are discretized on a time mesh, with

$$\frac{x_{n+1} - 2x_n + x_{n-1}}{\epsilon^2} + \left( \frac{\partial V}{\partial x} \right)_{x_n, y_n} = 0$$

$$\frac{y_{n+1} - 2y_n + y_{n-1}}{\epsilon^2} + \left( \frac{\partial V}{\partial y} \right)_{x_n, y_n} = 0,$$

where  $\epsilon$  is the time step and  $n = 0, 1, \dots, N-1$ . We impose periodicity by requiring that

$$(x_N, y_N) = (x_0, y_0)$$
$$(x_{N+1}, y_{N+1}) = (x_1, y_1),$$

with the period given by

$$\tau = N \epsilon.$$

For nonintegrable two-dimensional systems, the periodic trajectories form one-parameter families, and we find that it is especially convenient to make plots of  $E$  vs.  $\tau$ , where  $E$  is the energy and  $\tau$  is the period. Among the questions we wanted to answer were the following.

What is the topology of this plot? Is it like a tree? What about the branching behavior, in which the original trajectory generates new families? There are two types of branching:

- a) Isochronous branching, where the period does not change, and
- b) Period multiplying branching, where the new family or families have a period which is a multiple of the original period.

For studying periodic motion, two of the most important methods are

- a) the method of Poincaré sections,<sup>9</sup> which has been widely used in the literature, and
- b) the Monodromy method, which we have adopted.<sup>1-3</sup>

The method of Poincaré sections<sup>9</sup> has been particularly helpful in studying the behavior of nonlinear systems which are nearly integrable, i.e. close to where the KAM theorem applies.<sup>9</sup>

The Monodromy matrix is a  $4 \times 4$  matrix which describes the change in a trajectory after one period due to a small change in initial conditions.<sup>2,3</sup> Monodromy in Greek loosely means "once around the track".<sup>3</sup> The 4 dimensions of the matrix correspond to the  $x$  and  $y$  coordinates and their associated velocities or momenta. (We mention in passing that a variation of this method gives a formulation in terms of  $2 \times 2$  matrices, but this approach has never been implemented.) The eigenvalues of  $M$  (which are the Floquet-Lyapunov multipliers)<sup>9</sup> occur in pairs whose product is unity and two of them are always equal to one. The other two can be complex conjugates of one another ( $e^{+i\alpha}, e^{-i\alpha}$ ), in which case, the trajectory is stable, or they are ( $\pm e^{\gamma}, \pm e^{-\gamma}$ ) giving an unstable trajectory. The trace of the matrix gives its stability, and in the stable region we can have period multiplying which occurs when the stability angle is

equal to a rational fraction times  $2\pi$ . We feel that the Monodromy method is superior to that of Poincaré sections because it is a very fast method which can be used to thoroughly map out the entire phase space (even if the system is far from integrable) and because it works as well for unstable trajectories as it does for stable trajectories.<sup>1-3</sup> Also, the Monodromy method allows one to go very easily from one periodic trajectory to another in the same family or to a bifurcation from the original family.<sup>3</sup> Finally, the method can be used to calculate tori;<sup>12</sup> more about this later.

Figure 4 shows a schematic plot of the Trace (M) vs. E.<sup>2</sup> The places where it goes through 4 and 0 (denoted by 4 and Z) give rise to isochronous and period-doubling branchings, respectively. Above 4 and below 0 the family is unstable; in between it is stable and various branchings occur. Notice that these are double solutions, denoted by  $4^2$  and  $Z^2$  where the Trace (M) has a horizontal tangent. In reality, these can be two branchings which are so close together that they cannot numerically be distinguished from the tangency shown. In fact, it has been shown analytically that the  $4^2$  case consists of two, very close single branchings.<sup>4</sup> The point marked  $\bar{4}$  is a special case to be discussed later. On this plot it has a vertical tangent, while on the E- $\tau$  plot it has a horizontal tangent and is known as a "horizontal four."<sup>1,2</sup>

About five different potentials have been studied. The majority of my results today are from the so-called NELSON potential:<sup>1</sup>

$$V(x,y) = (y - \frac{1}{2} x)^2 + \frac{1}{2} \mu x^2, \mu = 0.1,$$

which consists of a deep valley in the shape of a parabola surrounded by

high mountains, as we see in the contour plot of Fig. 5. For this potential we were motivated by nuclear physics, where the deep valley could represent a collective degree of freedom coupled to other types of excitation. On this plot we also show the boomerang family of periodic trajectories. Notice that this family arises at small energies as a period doubling of the family of purely vertical oscillations. Other results that I will discuss were obtained using the MARTA potential<sup>2</sup>

$$V(x,y) = \frac{1}{2} x^2 + \frac{3}{2} y^2 - x^2y + \frac{1}{2} x^4,$$

which is a less symmetrical version of the celebrated Hénon-Heiles potential. As we see from Fig. 6, it is strikingly different from NELSON since it has two saddle points and goes to  $-\infty$  in some directions. Here we also show the boomerang family from MARTA, which again is very different from NELSON since it arises at small energies as the horizontal family of small oscillations. Figure 7 shows another important difference between NELSON and MARTA. MARTA has a family of oscillations which emanate from the saddle point.<sup>2</sup> Unlike the families which originate at small oscillations from the potential minimum, there can only be one saddle point family. This family is always unstable and does not branch into any other family.

Some calculations have also been performed with the Hénon-Heiles potential,<sup>9</sup> whose contours are displayed in Fig. 8. Notice that there are three saddle points. This potential, which is very famous, was first proposed in 1964 to model the orbits of stars around a galactic center. It is intriguing because it has a "triangular" symmetry, being invariant under rotations of  $120^\circ$  in the x-y plane. Moreover, all of

the potentials shown have symmetry under reflection of the  $x$  coordinate,  $x \rightarrow -x$ . This brings us to the general topic of symmetries.<sup>1,2</sup>

First, there are two kinds of trajectories:

a) Librations, in which the same path is traversed in both directions. The trajectory has well-defined turning points and is its own time-reversed trajectory.

b) Rotations, in which there is a closed path in one direction only. The opposite direction on the path gives the time-reversed trajectory, and it is a separate trajectory. On the  $E-\tau$  plots we label the rotations by the symbol  $\rho$ .

Now consider the reflection symmetry,  $x \rightarrow -x$ . There are again two possible classifications:

a) Trajectories which are symmetric about  $x = 0$ ; reflecting  $x$  does not give a new trajectory.

b) Asymmetric trajectories, which are not symmetric about  $x = 0$ . For each of these there is a companion trajectory obtained by reflecting the  $x$  coordinate. From now on, the terms symmetric and asymmetric refer to the symmetry about the  $y$  axis. Thus, for NELSON and MARTA we have four types of trajectories, taking into account the symmetries of time reversal and reflection:<sup>2</sup>

1. Symmetric librations (two symmetries)
2. Asymmetric librations (one symmetry)
3. Symmetric rotations (one symmetry)
4. Asymmetric rotations (zero symmetry).

We see that every asymmetric rotation always belongs to a quartet. One of the important contributions of our work has been to analyze both

numerically and mathematically the role that symmetries play during bifurcations.<sup>1,2,4</sup> Previously some work had been done by Meyer<sup>10</sup> on bifurcations for the so-called generic case, which means that no symmetries are present in the Hamiltonian. We have extended this work to include the two symmetries mentioned. Later in this report I will show several examples of how symmetries play a role when a family bifurcates, but I will not give a complete analysis of all of the cases that can occur.

I conclude this discussion of symmetries by showing in Fig. 9 an x-y plot of trajectories from the Hénon-Heiles potential.<sup>7</sup> The bottom-most trajectories marked with their  $\tau$  values illustrate the behavior of some members of the horizontal family at relatively low energy. Because of the triangular symmetry, each of these trajectories has two companion trajectories obtained by rotating the original trajectory by  $120^\circ$  and then by  $240^\circ$ . These are also displayed on Fig. 9. You can show numerically that each of the companion trajectories is a legitimate periodic solution for this potential.

### III. RESULTS

#### A. TOPOLOGY OF THE E- $\tau$ PLOTS

I will now discuss the main results of our work, with the principal emphasis on the NELSON potential.<sup>1</sup> Probably the most rational way to begin a study of periodic trajectories would be to go to the limit of small oscillations.<sup>3</sup> I might add that this is not how we actually got started. We discovered our first trajectories, more or less by just "having fun" with the early codes, and only later did we focus on the simplest families. However, an intelligent procedure would be to begin with the small oscillations solutions and to follow them to larger amplitudes, along with their bifurcations. Incidentally, the analogue in TDHF would be to start with the RPA solutions, whose continuations would give rise to large-amplitude collective motion. For the NELSON potential there are two families of small oscillations, one in the vertical direction, the other in the horizontal direction and their periods are not congruent. One of the interesting features of the vertical family is that if you continue it to larger amplitudes, it retains its harmonic behavior, with a constant period. However, as we see in Fig. 10, this is not true for the horizontal family.

Figure 10 shows an energy vs. period (E- $\tau$ ) plot of the vertical V and horizontal H families, as well as many other families.<sup>1</sup> This figure shows a number of features illustrating the general topology of E- $\tau$  plots, and we will return to it again later in this report. In general, this is a master plot of the most important or simplest symmetric

families. The circled capital letters give the major families; e.g. there are the vertical V and horizontal H families just discussed, and B is the boomerang family shown previously. Recall that B is a period doubling from the vertical family. P and Q are the beginnings of two asymmetric bifurcations. The dark lines indicate stable regions, while the thin lines denote instability. Sometimes small regions of instability and stability are indicated by u and s, respectively. The dark circles show very concentrated regions where the Trace (M) rapidly goes through 4's and zeros; such circles contain a tiny region of stability and perhaps an even smaller region of instability. Dot-dashed lines indicate various period-multiplying branchings, which are always period doublings unless otherwise indicated. The places where the Trace (M) goes through zero (Z) and 4 are so marked. Note the presence of 4's where the E vs.  $\tau$  curve has a horizontal tangent; we will later have more to say about 4's.

Figure 10 illustrates one very important feature, namely that a particular family may have more than one stable region.<sup>1</sup> Indeed, there may be an infinity of such regions. The B family, e.g., is stable at low energy, after which it has an extended region of instability; then at higher energy it again becomes stable, lasting apparently all the way to  $\infty$ . Similarly, the vertical family, which is stable at low energies, has recurring small regions of stability at higher and higher energies. This also shows that the "standard scenario," in which stability gets passed on by period doubling to successively more complicated trajectories, can miss a lot of the information.<sup>1</sup> We will have more to say about the standard scenario later.

Before discussing further the topology of the  $E-\tau$  plot, let us first show a few pictures of some of the symmetric families.<sup>1</sup> We begin with the A family which begins as a period quadrupling from the vertical family and ends at high energy as a period doubling from the same vertical family. This family is a symmetric libration, and Fig. 11 shows its behavior on an  $x-y$  plot in going from low to high energy. Notice that the higher energy trajectories have larger amplitudes, ending in a period-boudling from the vertical. Figure 12 displays separate  $x-y$  plots of various members of the C family, which is a symmetric rotation. This family begins at low energy as a period tripling from the vertical and at high energy it branches isochronously to the A family close to where the A family branches from the vertical. Figure 13 puts several of the previous  $x-y$  pictures of C together on a single plot.

We return now to a low-energy blow-up of our  $E-\tau$  plot in the vicinity of the horizontal ( H ) family.<sup>1</sup> In Fig. 14 we see the horizontal family plus the I and J families, the two symmetric families to the immediate right of H on the  $E-\tau$  plot. Note that the curve for H between  $h_1$  and  $h_2$ , if extended, seems to overlap roughly the curve for I between  $i_1$  and  $i_2$ . However, there are gaps between these families, and we have verified that these gaps are not numerical. These families are known as the "valley families" since in the lowest energy part of each curve the family occupies the valley of the potential and thus can be identified with the collective oscillations of nuclear physics. Let us see what happens. First, for  $\tau$  values  $\sim 20-22$ , the H family occupies the valley, but then it begins to climb the walls of the potential as the  $E-\tau$  curve abruptly makes a sharp turn upwards and backwards. About this point the

next family I comes down from the mountains and occupies the valley until  $\tau \sim 25.0$  when it also returns to the mountains. Then J takes over and repeats the same pattern. Figures 15 and 16 show the x-y plots of H and I at relatively low energies, and we see how the trajectories begin to leave the valley around  $\tau = 22.0$  and  $\tau = 25$ , respectively. Figure 17 is an x-y picture of two members each of the H, I, and J families when they are in the valley. The unshaded region is the valley, and the picture shows only the  $x > 0$  part since the librations are all symmetric about  $x = 0$ . Notice, too, that a new "hook" is added to the trajectory each time we switch to a more complicated valley family, and this feature is seen again and again with respect to other associations of families encountered on the E- $\tau$  plots. In any case, one sees that the situation is vastly more complicated than a single, continuous, collective family.<sup>1</sup> In fact, the valley trajectories are not part of a single continuous family, but rather are divided among sections of H, I, J, and presumably higher-order families beyond J.

You might ask yourself what happens to the horizontal family after it leaves the valley. The history of H is displayed in Fig. 18.<sup>1</sup> In the upper part of the figure we see that the family at low energy begins as a small horizontal oscillation, after which it grows until it reaches a maximum energy. The lower part of the figure shows the change in shape as the family decreases its energy until it branches as a period quadrupling from the vertical family. Returning to Fig. 10, we see the full behavior of the horizontal family.<sup>1</sup> Clearly, V and H are connected since H ends by branching onto V via period quadrupling. This could not happen for an uncoupled (integrable) Hamiltonian, for which the families

of small oscillations are independent of one another.

This perhaps is a good time to discuss additional general topological features of the  $E-\tau$  plots, which are nicely illustrated in Fig. 10.<sup>1</sup> First of all, there are only two ways a family can begin or end: (1) by branching upon another family, or (2) by becoming the family of small oscillations about an equilibrium point. In regard to (2), recall that for MARTA,<sup>2</sup> in addition to the H and V families, there is a family of oscillations emanating from the saddle point of the potential. Some families do not terminate anywhere, e.g. the V and B families go to infinity or they form closed curves (the I and J families). You may recall that one of the questions that we initially wanted to answer was whether the  $E-\tau$  plot is like a tree. Now we clearly see that the  $E-\tau$  plot is definitely not like a tree<sup>1</sup> since there can be many "cycles" like I and J which follow closed paths. Also, note that the long rotations in H, I, and J form cycles.

Finally, I and J are "islands," not obviously connected to the other families in the plot.<sup>1</sup> However, since I and J do give rise to period multiplying branchings, it is conceivable for large  $\tau$  that they could somehow connect up with the branchings from the other families. (This possibility seems remote, but it has not yet been investigated.) One other interesting feature of the  $E-\tau$  plot is that there is a symmetric rotation connecting the top and bottom parts of H, I, and J which are symmetric librations. This rotation is an isochronous branching, and we refer to it as a "rotation bridge" since it connects two very different parts of the cycle. In Fig. 19 we show the bridge for H. However, such bridges do not have to occur for cycles or islands, as we

see in Fig. 20. This rather unusual creature, obtained for the MARTA potential,<sup>2</sup> is an isolated asymmetric rotation. Recall that an asymmetric rotation has zero symmetry, which, it turns out, prevents it from branching isochronously.<sup>2</sup> We will have more to say about branching later, but for now we want to discuss further the topological differences between librations and rotations.

Figure 21 displays a detailed blow-up of the  $E-\tau$  plot in the vicinity of the V and B families.<sup>1</sup> This picture reveals a number of asymmetric branchings from these two families. The longer lines are librations and the shorter ones are rotations. This is typical of what one usually finds on the  $E-\tau$  plots.<sup>1</sup> Compared to the rotations, the librations are considerably more persistent, giving rise to many more branchings. Thus, it becomes natural to think of librations as the "more important" families, but I find rotations to be much more aesthetically appealing because of the beautiful way they form bridges between two very different librational shapes. Previously we saw such bridges connecting different parts of the same family (H, I, and J). Here the short rotational bridges connect different librations. On this plot I call your attention to two such rotations which have been carefully studied. The first is the "open boomerang" which branches from the boomerang (at  $E \sim 10.0$ ) and ends at the vertical family, thus connecting those two families. Another is the rotation marked  $\rho^*$  which serves as a bridge between two asymmetric librations. These two rotations are plotted in Figs 22 and 23, respectively. The heavy lines in Fig. 23 are the two "end" librations; note the difference in shape between these asymmetric librations.

Figure 24<sup>1</sup> shows again the relationship between rotations and librations. P and Q are two of the more important asymmetric librations which execute a large number of screw-like excursions in the  $E-\tau$  plane, keeping out of step with each other. (The dotted curves for parts of Q were not actually calculated, but are rough guesses based on our experience.) The net effect reminds one of a DNA molecule in two-dimensional projection. However, a whole series of rotation bridges connect P and Q at every half turn of the screw, e.g. the rotation shown which connects the point p2 on P with a point just above q2 on Q. This bridge is shown in Fig. 25. Notice the dramatic changes in shape of this rotation as it connects the two librations shown in the first and last frames.

In concluding this discussion of the topology of the  $E-\tau$  plots, I will discuss the small oscillation families of the Hénon-Heiles potential.<sup>7</sup> Figure 26 is an  $E-\tau$  plot of some of the more prominent families. Note again the presence of a saddle point family, S. Because of the extra symmetry, we see that there are three families which originate as small oscillations about the minimum of the potential. There are the usual V and H families, which are librations, and a totally new family, T which is a rotation. Also, all three families have the same period at small oscillations, but unlike NELSON or MARTA there is no family whose period remains constant as the energy is increased. Another interesting feature is that for small energies, V and T are stable, while H is unstable. Note, too, that as  $\tau \rightarrow \infty$  the vertical family approaches an asymptotic limit which is equal to the energy of the saddle point. The new rotational family T is plotted in x-y coordinates in Fig. 27. For small energies this trajectory is circular, while at higher energies, it

becomes triangular in shape; hence, the name T.

## B. BRANCHING BEHAVIOR

I now want to discuss the branching behavior of the families of periodic trajectories.<sup>1,2</sup> Of course, we have already talked about branching when we analyzed the topology of the E- $\tau$  plots since the two subjects are intimately related. However, our focus here will be on how, why, and when the branchings take place.

One of the first, very obvious points about branching is that at the branching point the original and the new family (or families) coalesce (which explains why the Trace (M) goes through 4 for the isochronous case). First, consider isochronous branchings (when the period doesn't change). Imagine such branchings from, say, a boomerang-shaped curve, which is a symmetric libration. In one case you might get, e.g., the open boomerang which is a symmetric rotation or in another, the asymmetric boomerang. In both cases we note that the original trajectory has lost one of its symmetries, and, as we have mentioned before, symmetries play a crucial role in determining branching behavior.<sup>2,4</sup>

The second type of branching occurs when we bifurcate to a trajectory whose period is a multiple of the original trajectory. We have seen a number of examples of such branchings. Recall, e.g., that the vertical family gives rise to two important period quadruplings:<sup>1</sup> One is the A family; the other, the H family. Both branchings take place at the same point, and we thus uncover another important result: sometimes two new families arise at a bifurcation point.<sup>1,2,4</sup>

From Fig. 21 we see that there are four important simple branchings

from the boomerang family:<sup>1</sup> at low energy, a  $Z^2$  and a 4 and again at high energy a 4 and a  $Z^2$ . These branchings are shown in Fig. 28, and, going clockwise starting with the upper right frame, we have: the double open boomerang (a symmetric rotation from the lower  $Z^2$ ), the asymmetric boomerang (lower 4), the open boomerang (upper 4), and the double mushroom (a symmetric rotation from the upper  $Z^2$ ). For the double open boomerang, we only show one trajectory; for each of the other cases, we display several trajectories. Also, the  $Z^2$  cases are double solutions. Thus, for each of these we have another, companion solution which is an asymmetric libration. Figure 29 displays a clover-leafed isochronous branching from a U-shaped family for the MARTA potential.<sup>2</sup> These are all relatively simple bifurcations. However, in general, the period-multiplying trajectories can become exceedingly complicated. For example, Fig. 30 is an x-y plot of a single trajectory obtained from a period doubling of the I family.<sup>1</sup>

Without going into much detail, let us now indicate some of the rules for branching.<sup>2</sup> When we first started this work, there seemed to be two or even three types of possible isochronous branchings, where the Trace (M) went through a value of 4. In the first case (4), we were easily able to find the new family as the original family went through the bifurcation point, and this always seemed like the "standard branching." However, there were other cases where the Trace (M) went through 4, but at a place where the family had a horizontal tangent in the E- $\tau$  plane.<sup>1</sup> These are known as "horizontal fours" ( $\bar{4}$ 's), which I have previously called to your attention. In any case, in the early days of our work it always seemed as if the  $\bar{4}$ 's were very strange, special, probably

somewhat rare creatures since, as far as we could determine, no branching took place. In fact, after some very careful work, we were able to establish<sup>1,2</sup> (both numerically and analytically) that no branching could take place at a  $\bar{4}$ . Also, at a  $\bar{4}$  the trajectory always switched from stable to unstable, or vice versa. Moreover,  $\bar{4}$ 's were much more common than we originally thought, and in addition, a  $\bar{4}$  turns out to be the generic case (i.e. what one encounters in the absence of any symmetries).<sup>10</sup> The other isochronous branchings, at the  $4$ 's on the  $E-\tau$  plot, occur only when symmetries are present, and this too is an important result of our work.<sup>1,2</sup> The only kind of trajectory which cannot have an isochronous branching is an asymmetric rotation, which has no symmetry.<sup>2</sup> On the other hand, the  $4^2$  case<sup>1</sup> indicated on the  $E-\tau$  plots (the third kind of isochronous branching) occurs for a symmetric libration, which has two symmetries. (Recall, however, that  $4^2$  is only approximate; in reality, this is two very closely spaced  $4$ 's.<sup>4</sup>)

The next point is that at a branching point, there is a kind of "conservation of stability,"<sup>1</sup> but we must define precisely what we mean by this expression. We use the Poincaré section for our dynamical system and define a "Poincaré index" as follows. For every elliptic (stable) fixed point of the Poincaré wave one assigns the index  $\sigma = +1$ , while for every hyperbolic (unstable) fixed point one assigns the index  $\sigma = -1$ . The total Poincaré index, for a particular energy at a branching point, is the sum of all of the individual  $\sigma$ 's, and this remains conserved as energy is varied through a branching. I.e., what is conserved is "stability minus instability." In applying this rule, it is very important to take into account the symmetry of the bifurcation point.<sup>2</sup>

E.g., consider the point (4) marked  $\beta$  in Fig. 14. For energies below  $\beta$  we have one asymmetric trajectory, a symmetric libration, giving  $\sigma = -1$ . Above  $\beta$ , the original trajectory has now become stable, with  $\sigma = +1$ . However, there are two unstable asymmetric librations (obtained by letting  $x \rightarrow -x$ ), each with  $\sigma = -1$ , so that the net  $\sigma$  is  $-1$ . Thus, stability is conserved. Similarly, at the 4 just below  $\beta$ , the main trajectory switches from stable to unstable, but the branching is to a stable symmetric rotation (with two trajectories for the two directions), so  $\sigma(\text{net}) = +1$  both below and above the branching. Also, consider the  $4^2$  branching, for which the main trajectory maintains its stability. However, there are four branching trajectories: two stable symmetric rotations and two unstable asymmetric librations, so once again stability is conserved. (This last example is really the same as the two previous cases, with the distance between them becoming very small.<sup>4</sup>)

The rule for branchings has profound implications for period multiplying branchings.<sup>1,2,4</sup> We will not have time to treat this subject in any detail, but let us indicate several of the main results. For period doubling, which occurs whenever the Trace (M) goes through zero (Z), there is only one new family. However, for a double solution ( $Z^2$ ) there are two new families. Then, two new families also arise for all period multiplying bifurcations greater than 2; i.e. for period tripling, period quadrupling, etc. Again the exact nature of the branching depends upon the symmetries present at the bifurcation point.<sup>2,4</sup>

One other result about bifurcations is worth mentioning. So far, we have encountered cases where the two new families (one of which is stable, the other, unstable) emerge on the same side of the branching;

i.e. both increase or decrease in energy. However, it is also possible for one of the two to go up in energy, the other down in energy.<sup>1,2,4</sup> This type of behavior can occur for  $Z^2$  period doublings<sup>4</sup> and for higher-order period multiplyings (e.g., tripling<sup>1,2</sup> and quadrupling<sup>2</sup>). When this happens, both new families are always unstable.<sup>1,2,4</sup> Figure 31 shows a period tripling of the asymmetric boomerang.<sup>1</sup> The original trajectory is shaded and the new families emerge at the 4.00 point, one in each direction. The original trajectory is stable both above and below the branching point, while each of the new families is unstable. Thus, once again stability is conserved. However, the lower family rapidly goes through a  $\bar{4}$  (with, of course, no branching) and becomes stable, after which its energy increases. Then Fig. 32 displays x-y pictures of the original trajectory at the bifurcation point (left) and the two new trajectories (middle and right). The middle and right pictures are taken somewhat beyond the region shown in Fig. 31 in order to distinguish the details of these two trajectories. Notice that the symmetry does not change. The original family is an asymmetric libration, as are both of the new families. However, there are many examples of period multiplying bifurcations where the symmetry does change.<sup>1,2</sup>

#### IV. NONPERIODIC TRAJECTORIES

Let us briefly study some nonperiodic trajectories in order to show that periodic and chaotic phenomena are intimately related. The NELSON potential<sup>1</sup> is particularly suited for this analysis because it has no saddle points and always goes asymptotically to + infinity in any direction. Thus, for any energy all trajectories remain in a finite region of phase space and are therefore "recurrent."<sup>9</sup>

Figure 21 is an  $E-\tau$  plot containing the boomerang family,<sup>1</sup> which has the simplest nontrivial periodicity. We will examine a nonperiodic trajectory which lies very close in phase space to a periodic trajectory. The nonperiodic trajectory is obtained by varying just slightly the coordinates of two adjacent points on the periodic one. There are three points in phase space that we will consider. The first point is taken from the lower stable region, close to where the boomerang branches form the vertical family. The second point is right in the center of the unstable middle region. The third point is on the upper stable branch somewhat above the point where the branching to the open boomerang takes place.

The nonperiodic trajectories for each of these cases are shown in Figs. 33, 34, and 35, respectively.<sup>1</sup> There are clearly very pronounced differences between the nonperiodic trajectories obtained from the stable and unstable regions.<sup>1</sup> For both of the stable cases, the trajectory has an envelope shaped like and surrounding the original boomerang. Such trajectories remain on a two-dimensional torus in phase space and

have been called regular or quasiperiodic.<sup>9</sup> In contrast, the nonperiodic trajectory from the unstable region starts out near the boomerang, but very soon leaves it and wanders more or less at random in the valley of the NELSON potential. Clearly, it lies in a chaotic region in phase space. There is another difference between the two types of trajectories.<sup>1,9</sup> Since a quasiperiodic trajectory remains on a torus, its velocity vector at any particular point of x-y space can only have one of two directions, thus giving rise to a "cross-hatched" pattern which is particularly evident in Fig. 35. On the other hand, the chaotic trajectory does not lie on a torus, so that the velocity vector can be in any direction.

The number of time steps for the chaotic trajectory in Fig. 34 is 5000. Figure 36 shows the effect of doubling the number of time steps, while Fig. 37 is a blow-up of Fig. 36 in the vicinity of the origin. We note in passing, too, that such quasiperiodic and chaotic trajectories were previously studied by Michael Hénon in connection with a restricted three-body problem.<sup>9</sup>

## V. CALCULATION OF INVARIANT TORI

Finally, we mention a very interesting development in the research program. It turns out that the Monodromy method can be extended to the calculation of invariant tori for a nonintegrable system.<sup>12</sup> Of course, as we have just seen in the previous discussion, periodic orbits can always be used to study the phase space in which they are imbedded. What is new about the Monodromy extension is that actual periodic trajectories become approximations for the nearby tori in phase space (which is assumed to be not too chaotic). These trajectories are called "quasi-tori." One important result of this work is that a family of tori can connect distinct families of periodic trajectories.

The method that has been developed allows one to calculate a periodic trajectory by varying both its energy and its winding number, which is defined in terms of the two eigenvalues of the Monodromy matrix that are not equal to 1. That is, for a stable trajectory we have

$$e^{+i\alpha}, e^{-i\alpha}$$

and

$$\alpha = 2\pi \frac{b}{m},$$

where  $m$  and  $b$  are integers. For these values of  $\alpha$  you get bifurcations of order  $m$ . The winding ratio is then given by

$$\rho = \frac{b}{m},$$

and the trick is to take rather large values for  $m$ , so that the bifurcated trajectory loops many times around the original or parent

trajectory. This behavior is nicely illustrated in Fig. 38,<sup>12</sup> where we show a periodic trajectory with  $\rho = 23/47$  for the horizontal family H of MARTA. In (a) we allow the computer to draw lines between points which emphasizes the whole orbit; the cross-hatched behavior is identical to that of the nonperiodic, regular trajectories displayed in the last section. However, in (b) we just show the points as they occur, and you see that they group themselves into planes which are perpendicular to the parent trajectory. In Fig. 39<sup>12</sup> we show another periodic trajectory representing a torus; for this case  $\rho = 64/107$ .

We remark, too, that another reason for focusing on the periodic trajectories with large  $m$  values is that these  $\rho$  values are precisely the rational ratios which are "least affected" by the KAM theorem. I.e., the KAM theorem tells us that when a torus pertaining to a rational ratio of frequencies is destroyed, some small fraction of nearby irrational tori are also destroyed and this fraction decreases as the rational ratios become less simple. Thus, for large  $m$ , the bifurcated periodic trajectory should approximate very well the tori in that part of phase space.

Finally, Fig. 40<sup>12</sup> shows a number of pictures of the bottom family of MARTA. Here a family of tori connect the horizontal and vertical families, as you can see in going from right to left. Each row of the figure is for a distinct energy, which are .05, .08, .11 in going from top to bottom. For each column of the figure, we have a constant winding number; the two columns on the left have relatively simple winding numbers. You can see how these quasitori vary with energy and winding number. It is interesting that even though  $V$  becomes unstable

at an energy of .1, quasitori for the bottom family still exist at an energy of .11.



## VI. CONCLUSIONS

Recently some very important studies in classical nonlinear dynamics have been completed. In this work, periodic motion in two-dimensional nonintegrable systems has been carefully analyzed. The most important results can be summarized as follows.

(1) A new algorithm has been developed for calculating the classical periodic trajectories. It is called the Monodromy method, and it is superior to the more conventional method of Poincaré sections for several reasons. First, it can be used to map out thoroughly the entire phase space, and it enables one to calculate unstable periodic trajectories as easily as the stable ones. Next, starting with a given periodic trajectory, one can very easily find another trajectory in the same family or in a new family which bifurcates off of the original family. Finally, the Monodromy method can be used to calculate the invariant tori of nonintegrable systems.

(2) A wealth of numerical data has been obtained, giving a rich variety of librational and rotational motion. (About 5000 trajectories comprising roughly 50 families have been studied.)

(3) It has been especially convenient to present the data in the form of energy vs. period ( $E-\tau$ ) plots. These plots have very interesting topological properties which nicely reflect new features of the underlying dynamical motion.

(4) Very careful numerical and analytic studies have been made regarding the branching or bifurcation behavior of the families of

periodic trajectories. This includes both isochronous branching (in which the period of the new family is the same as that of the parent family) and period-multiplying bifurcations (in which the period of the new family is a multiple of the period of the parent). One of the main results has been to show how symmetries (e.g., time-reversal and reflection) affect the details of the branching.

(5) The stability of the periodic trajectories determines the behavior of the phase space in which they are imbedded. Stable trajectories lie in regular regions of phase space, while unstable trajectories lie in chaotic regions.

(6) Tori can also be studied using these methods. Periodic trajectories with highly winding orbits are good approximations to the invariant tori which lie nearby in phase space. It has been shown that families of such "quasitori" can connect two different families of periodic trajectories.

(7) Finally, this work has great promise of being extended to TDHF theory in nuclear physics. To understand the connection between the classical studies and TDHF, it is instructive to consider how one initiates the classical calculations when no periodic solutions are known. The logical way of beginning is to find first the families of small oscillations about the equilibrium points of the potential. When at least one trajectory from each of these families is known, one can use the Monodromy methods to go to larger amplitudes for each family and, in addition, to find many new families. (However, as we have seen, there are collections of families which appear to be not connected to the families of small oscillations or, indeed, to any other families. Then

special methods must be used to locate such families.) The analogue in TDHF would be to start with the RPA solutions and use generalized Monodromy methods to generate solutions of large amplitude collective motion. (The isolated families will again have to be found using special techniques.) Thus, small and large amplitude collective motion will be mapped out in TDHF just as it was in the classical case. Such a study will be very useful in nuclear structure and eventually in heavy-ion reactions (see Figs. 1, 2, and 3).



## VII. REFERENCES

1. M. Baranger and K.T.R. Davies, Ann. Phys. (N.Y.) 177, 330 (1987).
2. M.A.M. de Aguiar, C. P. Malta, M. Baranger, and K.T.R. Davies, Ann. Phys. (N.Y.) 180, 167 (1987).
3. M. Baranger, K.T.R. Davies, and J. H. Mahoney, Ann. Phys. (N.Y.) 186, 95 (1988).
4. M.A.M. de Aguiar and C. P. Malta, Physica D 30, 413 (1988).
5. W. C. Saphir, B. S. thesis (M.I.T., Cambridge, MA, 1986), to be published.
6. M. A. Kagarlis, B.S. thesis (M.I.T., Cambridge, MA, 1986), to be published.
7. T. Huston, unpublished.
8. S. E. Koonin, "Computational Physics," (Benjamin/Cummings, Menlo Park, CA, 1986), pp. 33-34.
9. M. Hénon, in "Chaotic Behavior of Deterministic Systems - Les Houches 1981," (G. Iooss, P.H.G. Helleman, and R. Stora, Eds., North-Holland, Amsterdam, 1983), p. 53.
10. K. R. Meyer, Trans. Am. Math. Soc. 149, 95 (1970).
11. M. R. Strayer, R. Y. Cusson, A. S. Umar, P.-G. Reinhard, D. A. Bromley, and W. Greiner, Phys. Letts. B135, 261 (1984); A. S. Umar, M. R. Strayer, R. Y. Cusson, P.-G. Reinhard, and D. A. Bromley, Phys. Rev. C 32, 172 (1985); A. S. Umar, Ph.D. thesis, Yale University, 1985 (unpublished); A. S. Umar and M. R. Strayer, Phys. Lett. 171B, 353 (1986); M. R. Strayer, "The

Time-Dependent Hartree-Fock Method and Chaos in Nuclear Dynamics,"  
Proceedings, Symposia of the A.P.S. Topical Conference on Few-Body  
Systems and Multiparticle Dynamics, Crystal City, Virginia, April  
20-24, 1987.

12. M.A.M. de Aguiar and M. Baranger, Ann. Phys. (N.Y.) 186, 355  
(1988).

## FIGURE CAPTIONS

Figure captions are not included since the figures are explained in the text.



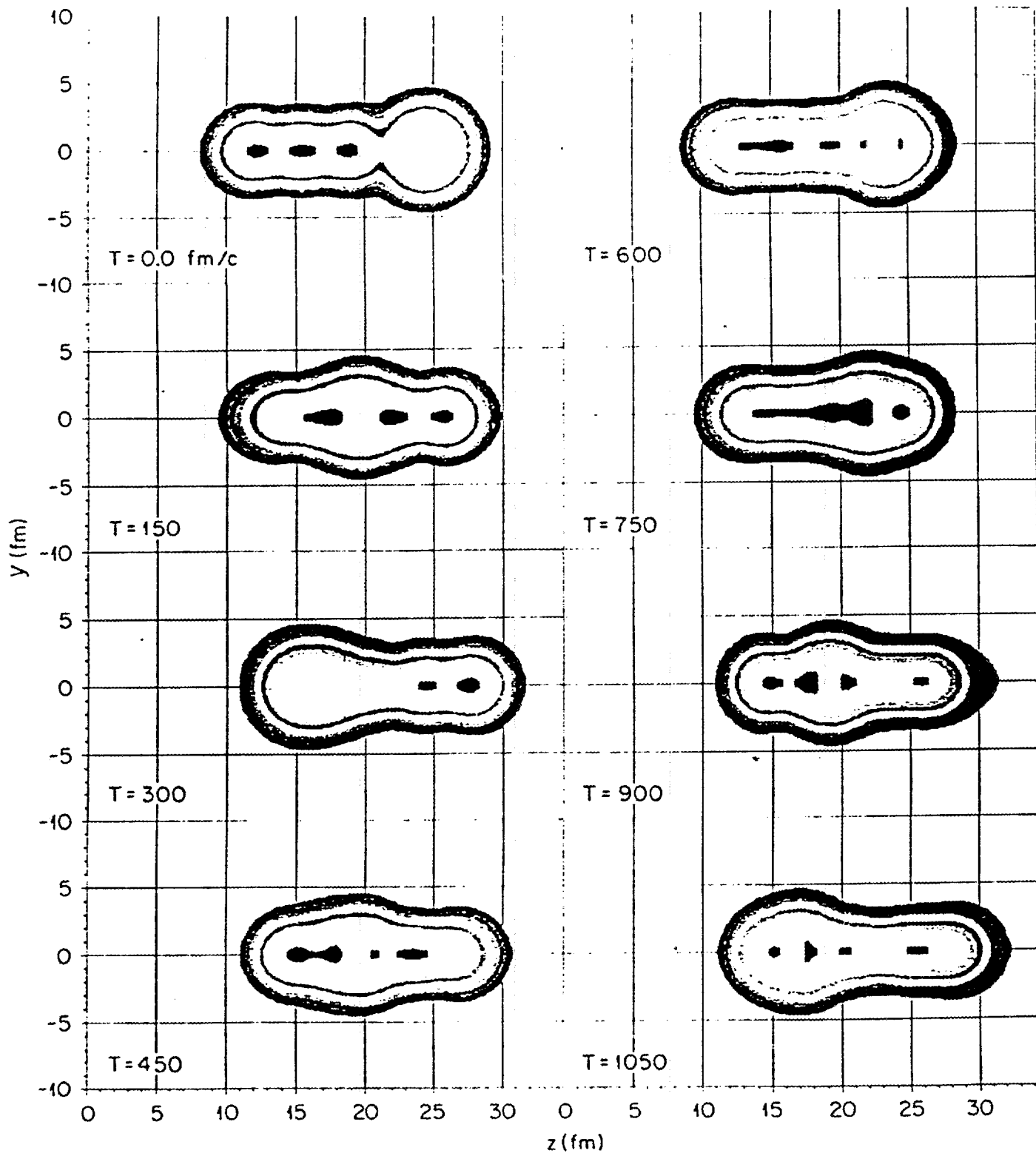


Fig. 1

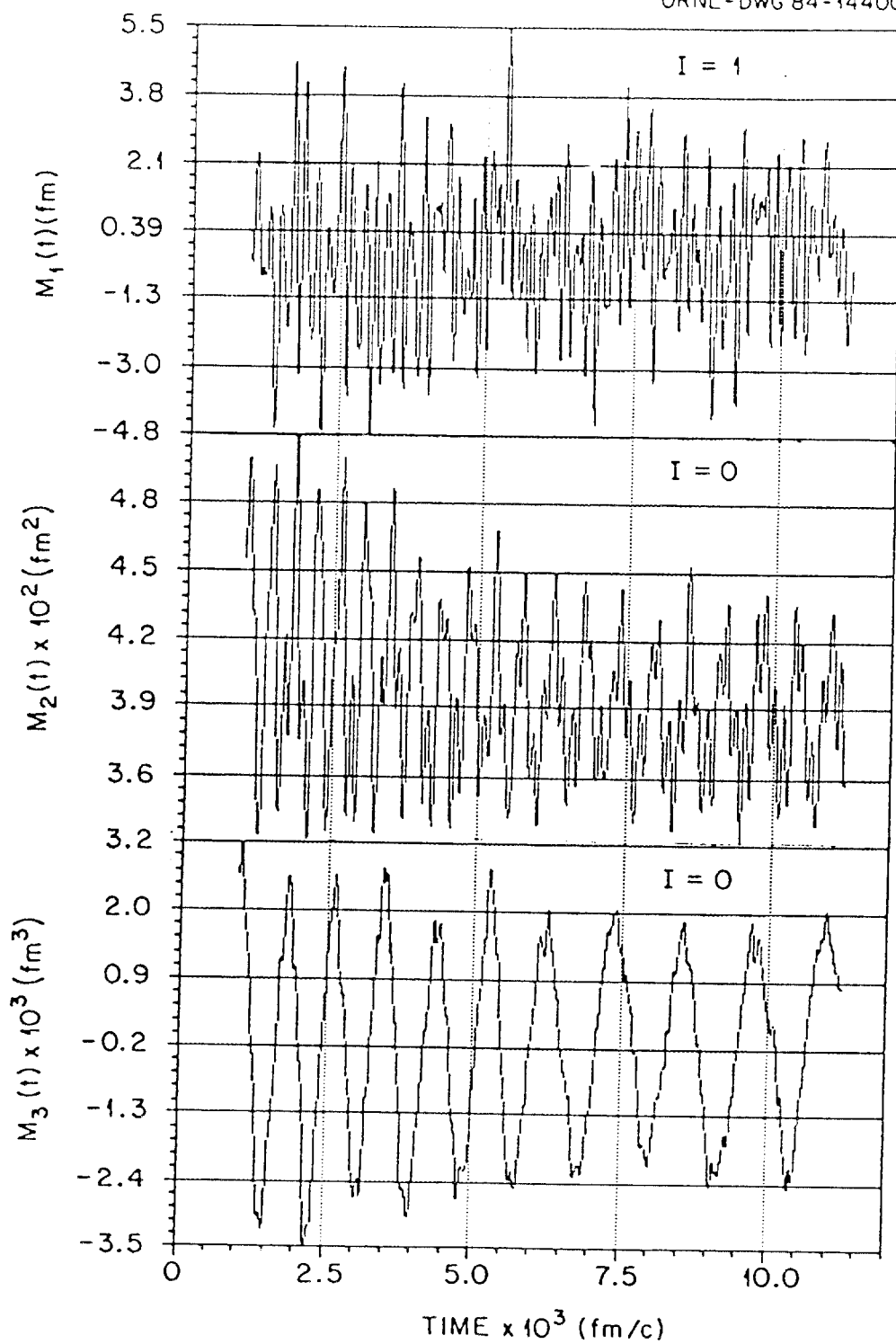


Fig. 2

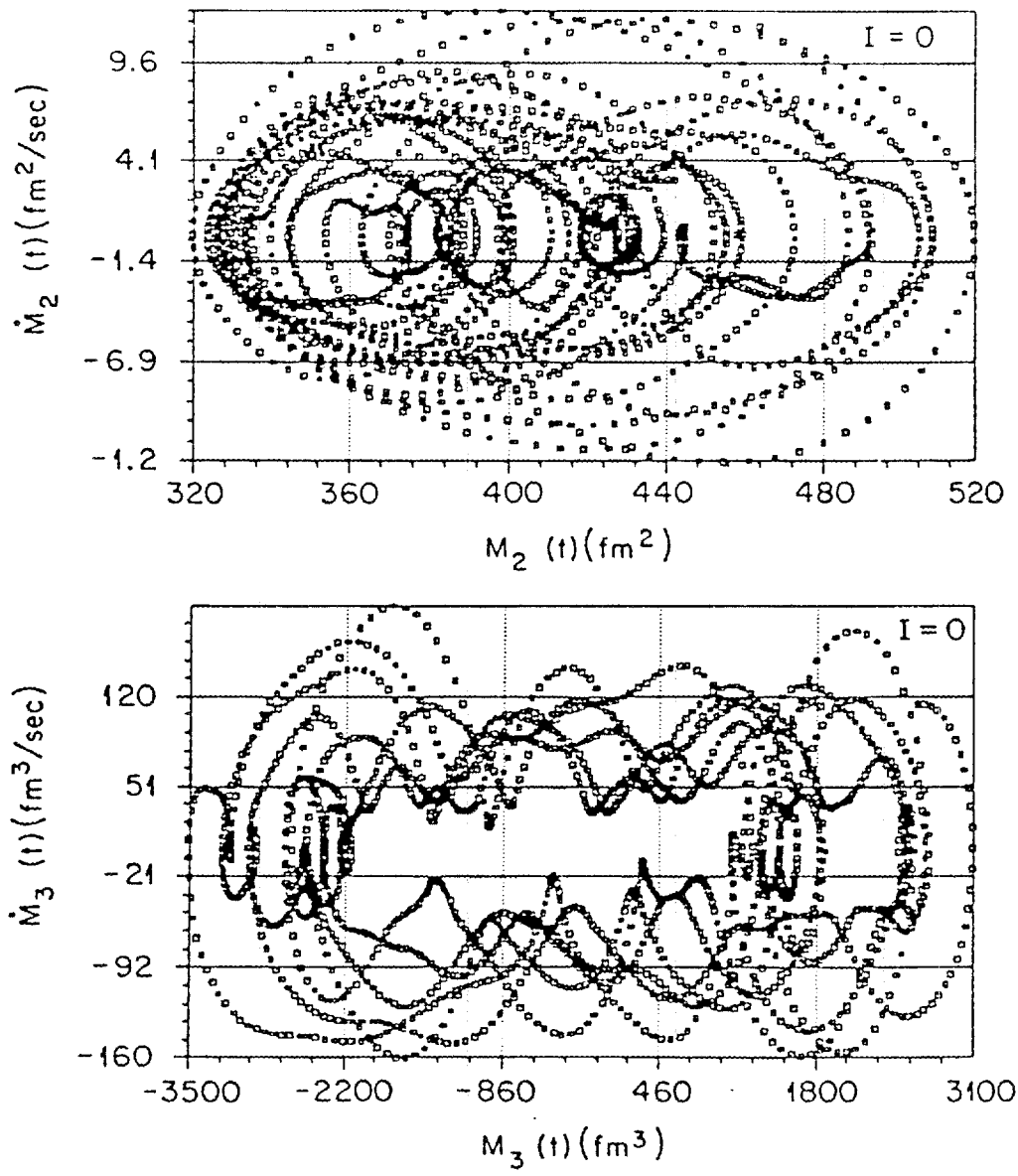


Fig. 3

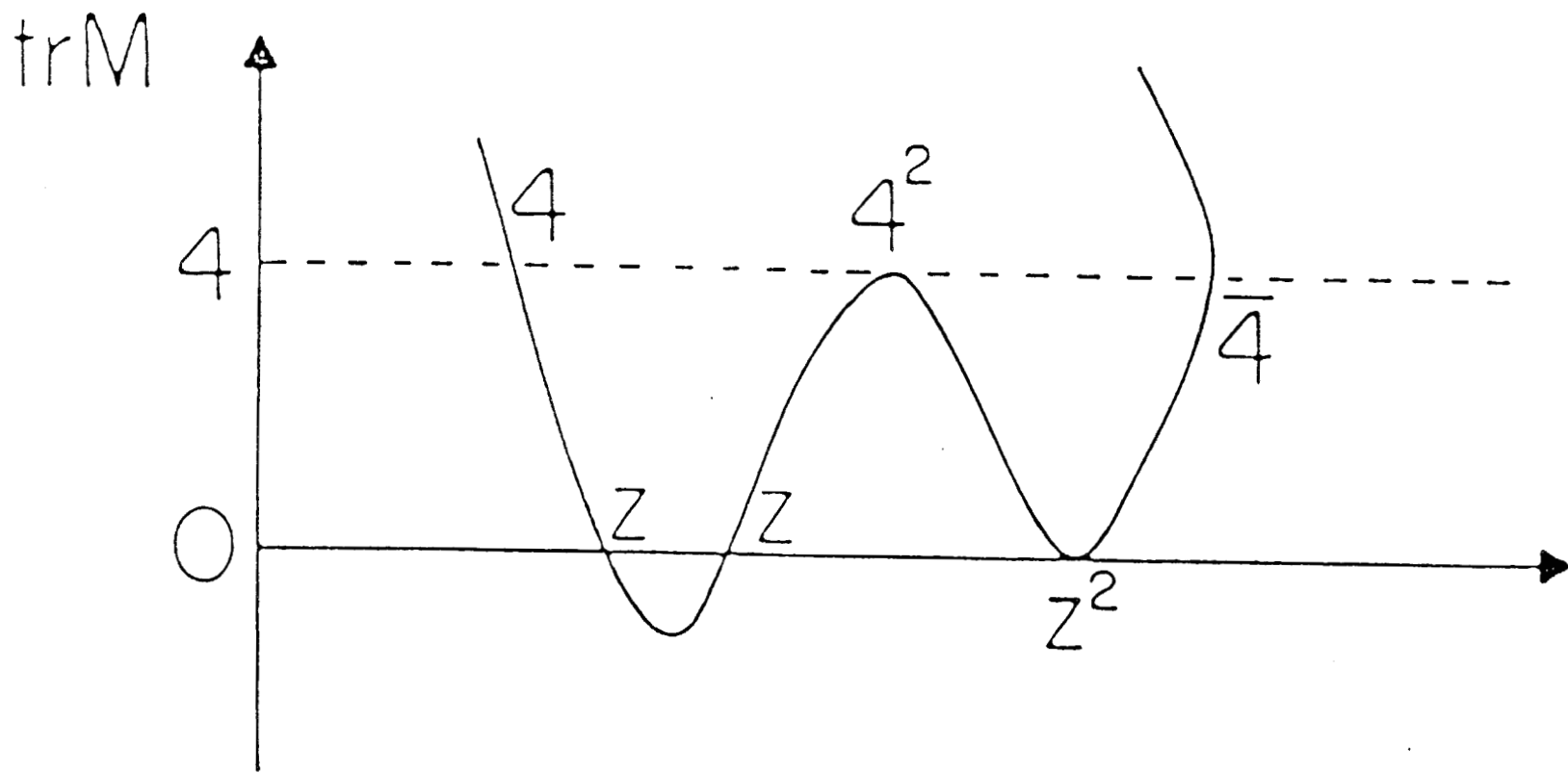


Fig. 4

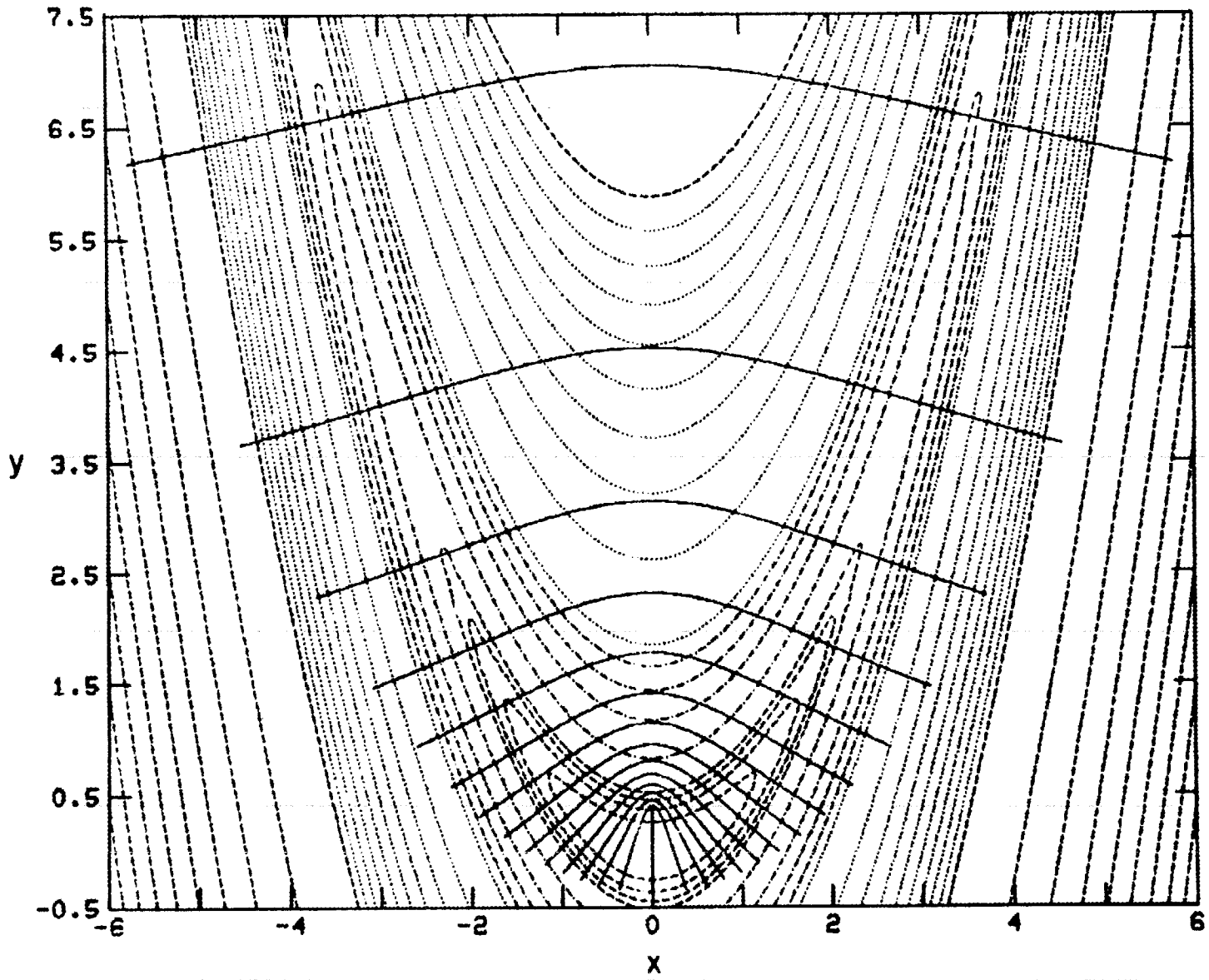


FIG. 5



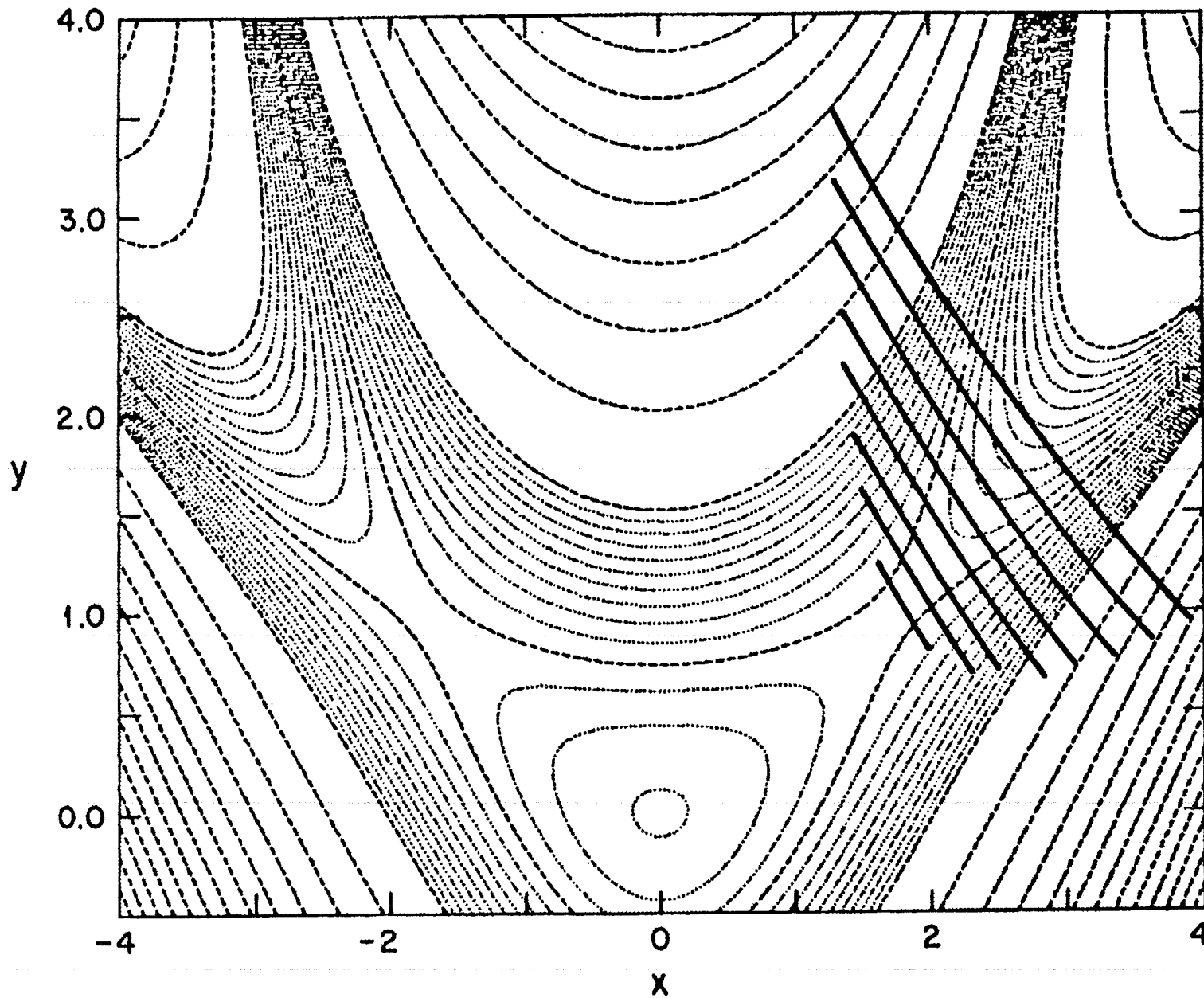


FIG. 7

FIG. 8

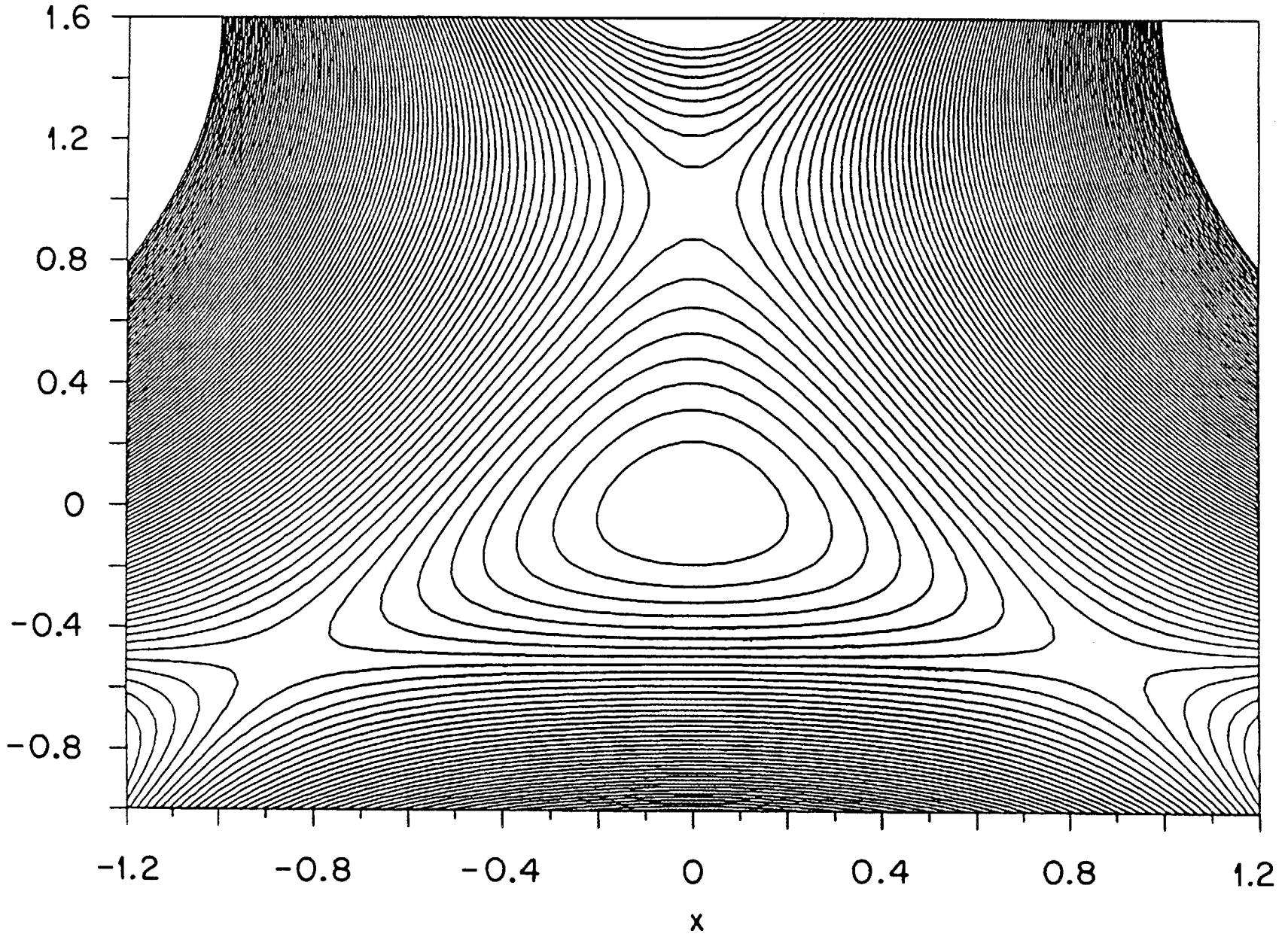
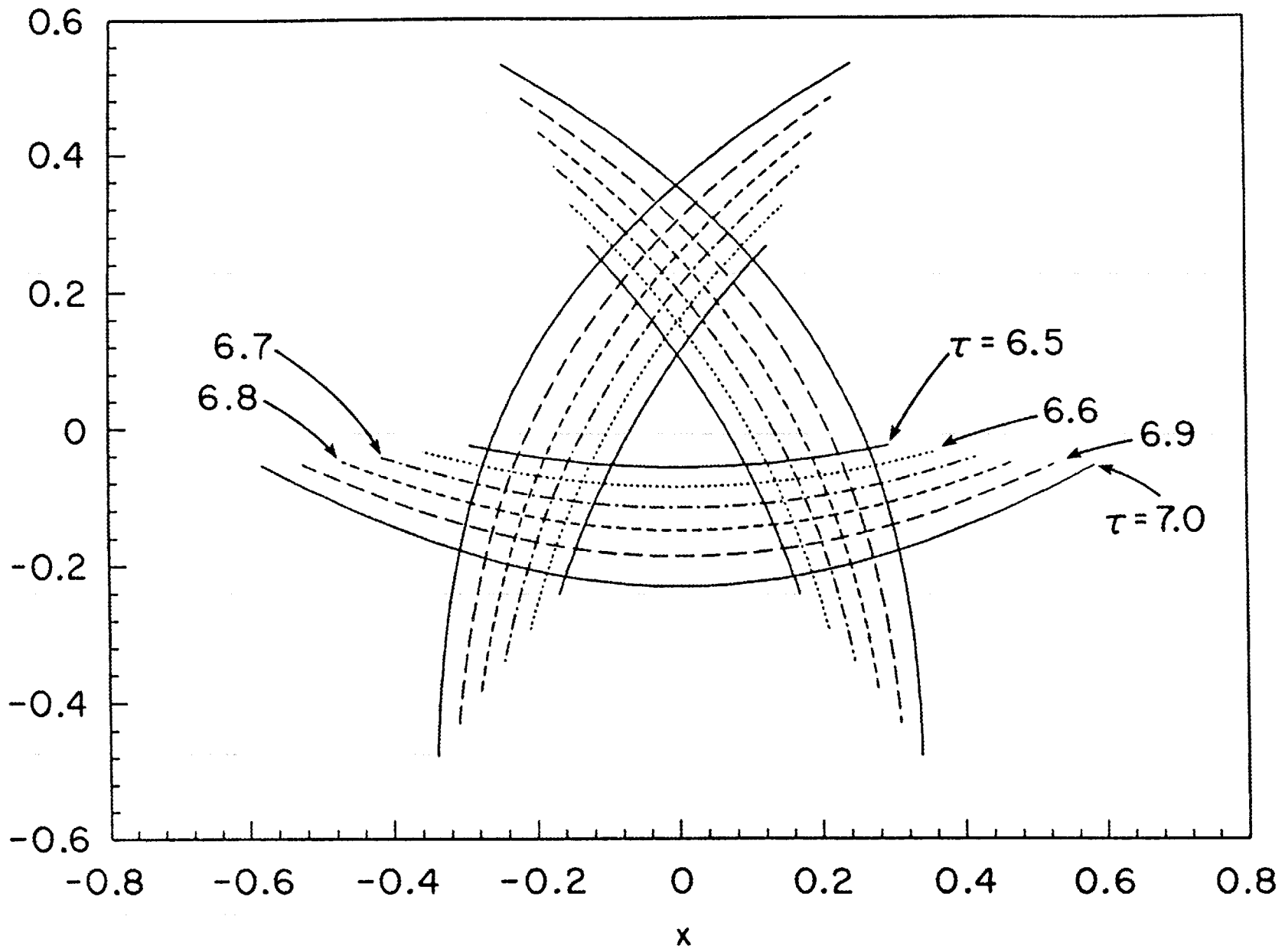


Fig. 9





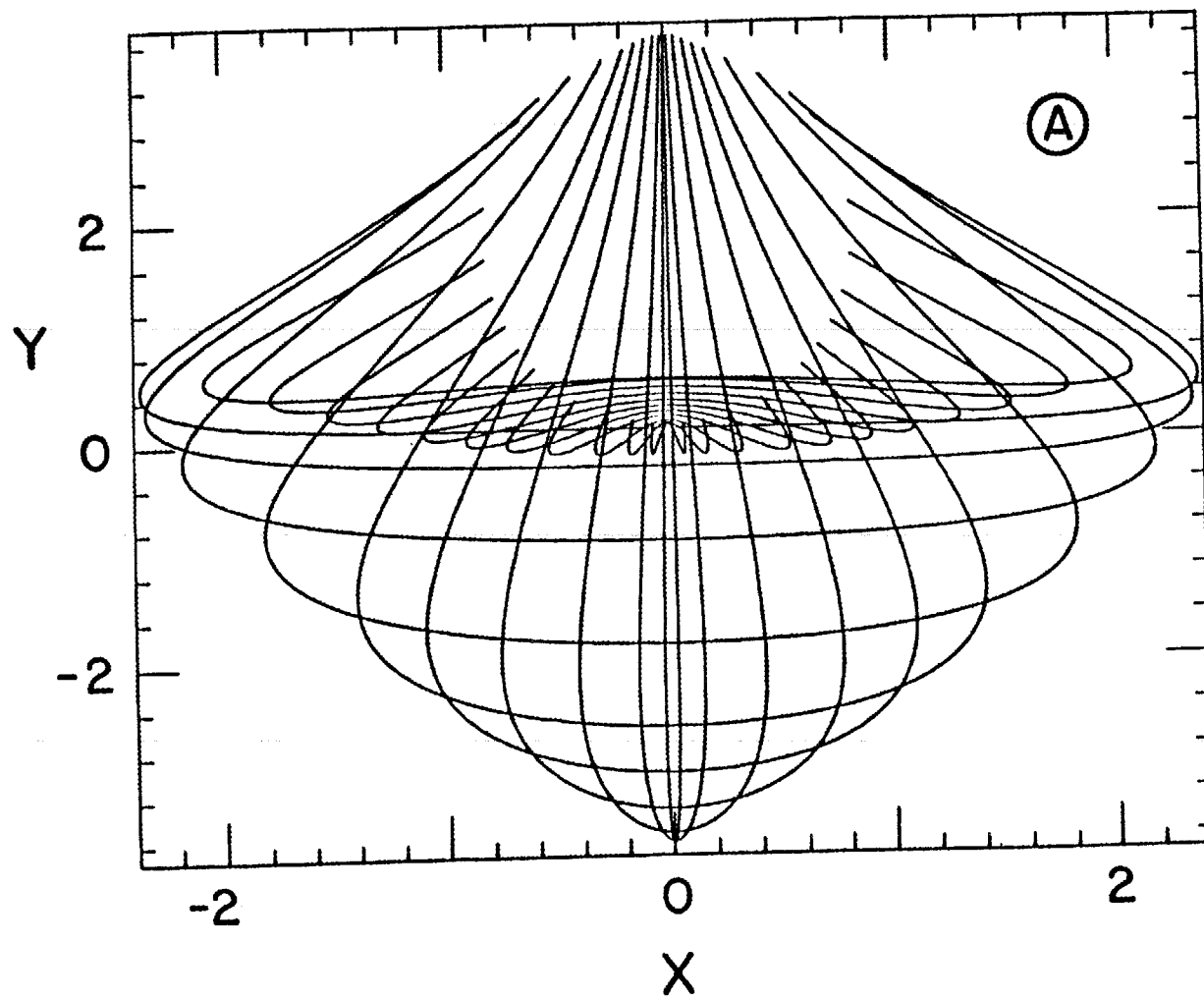
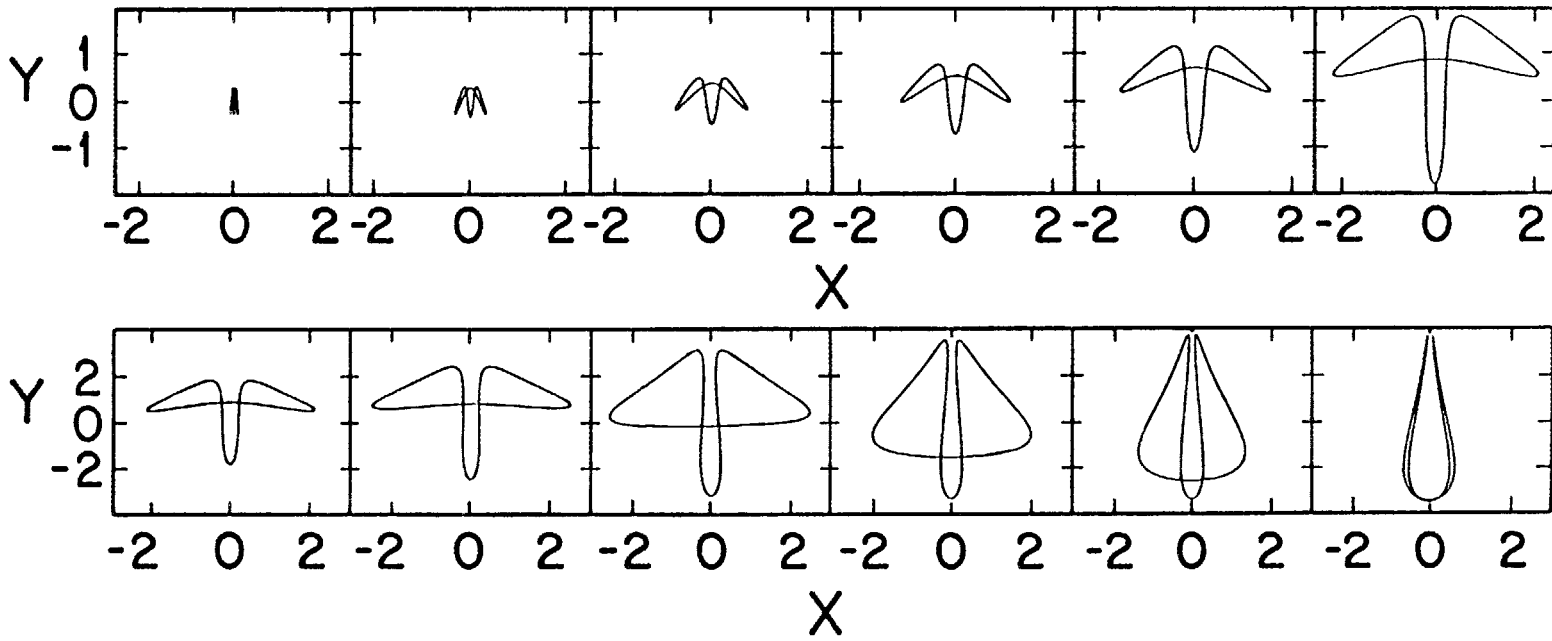


Fig. 11

Fig. 12



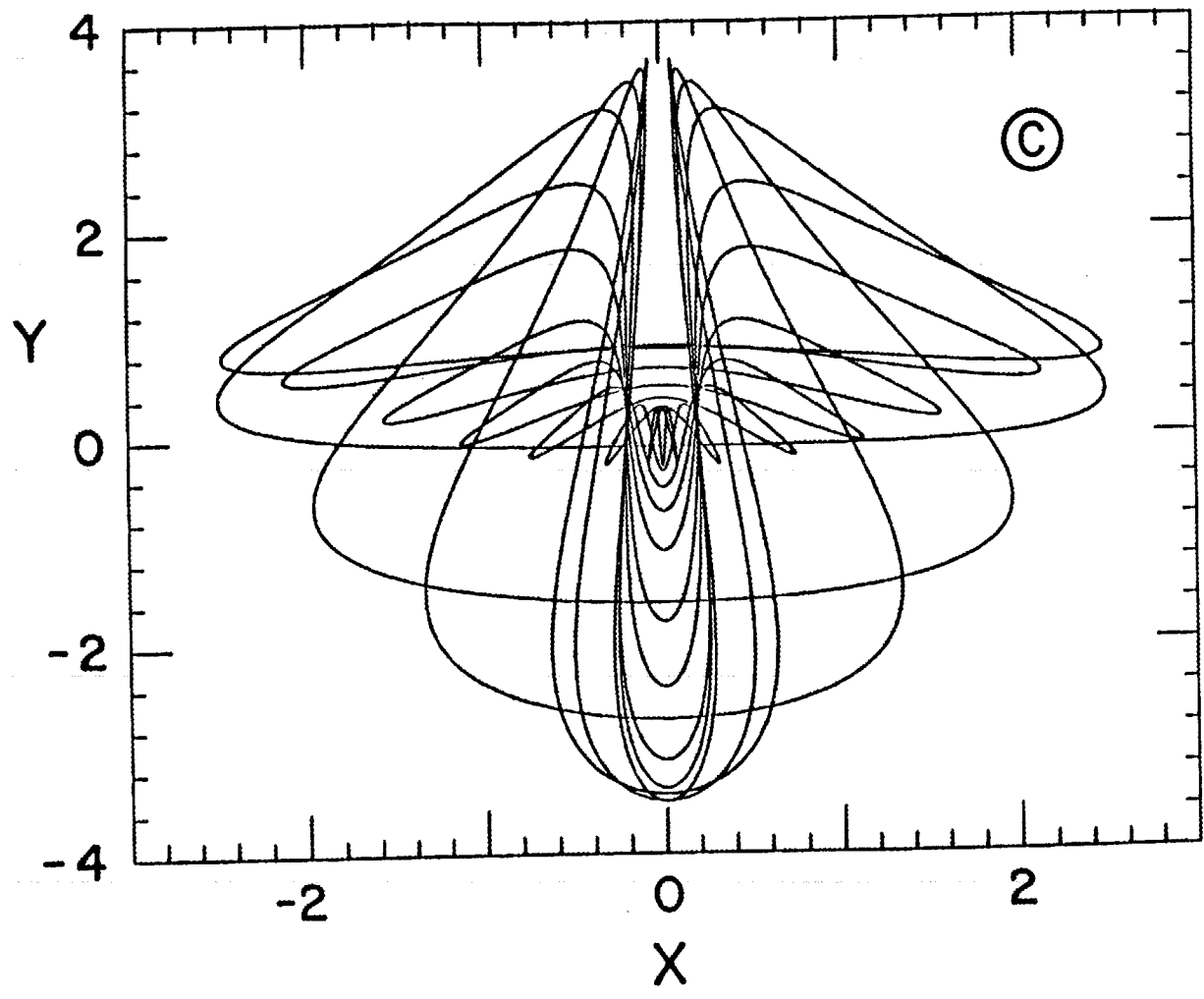


Fig. 13



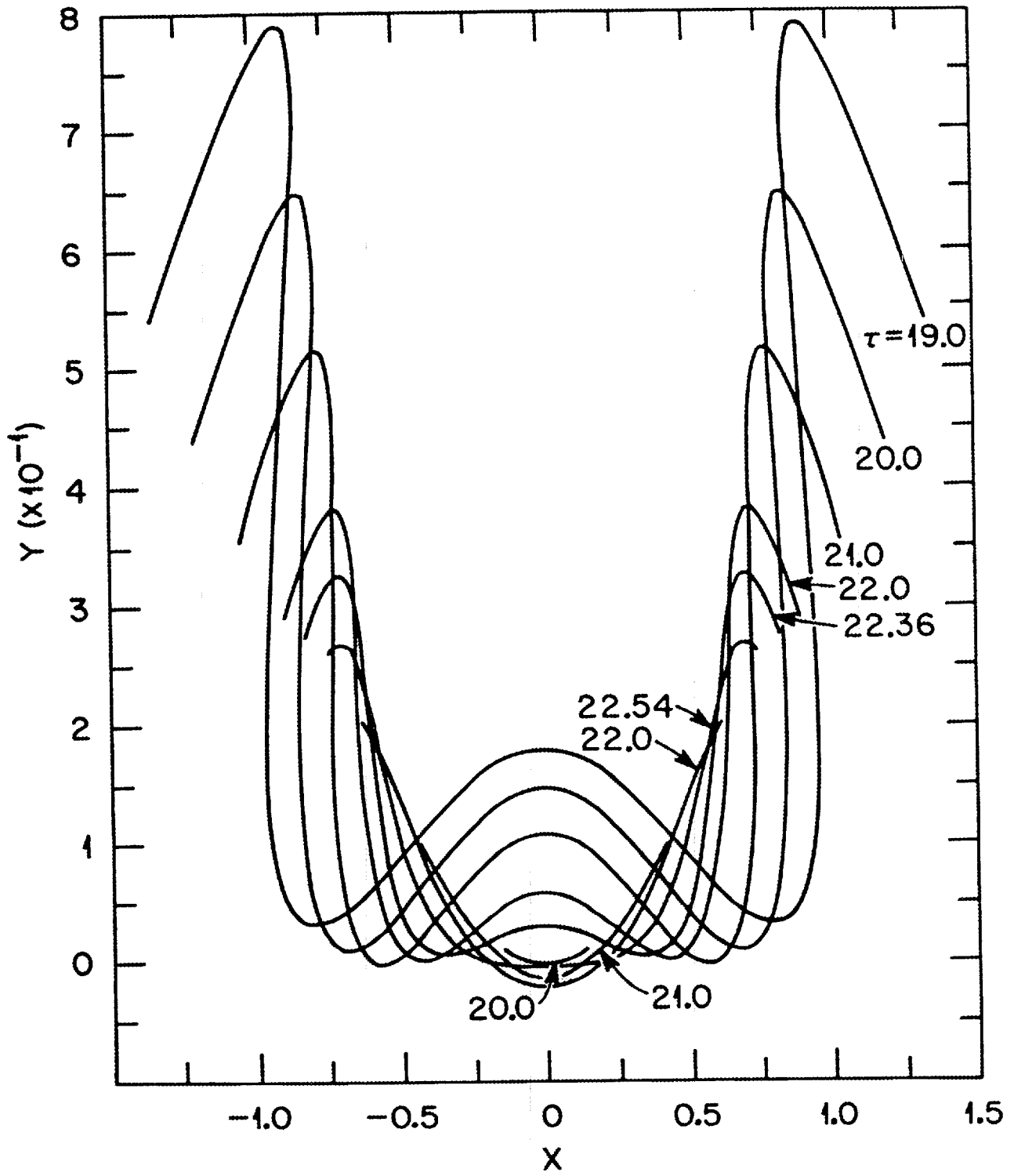


Fig. 15

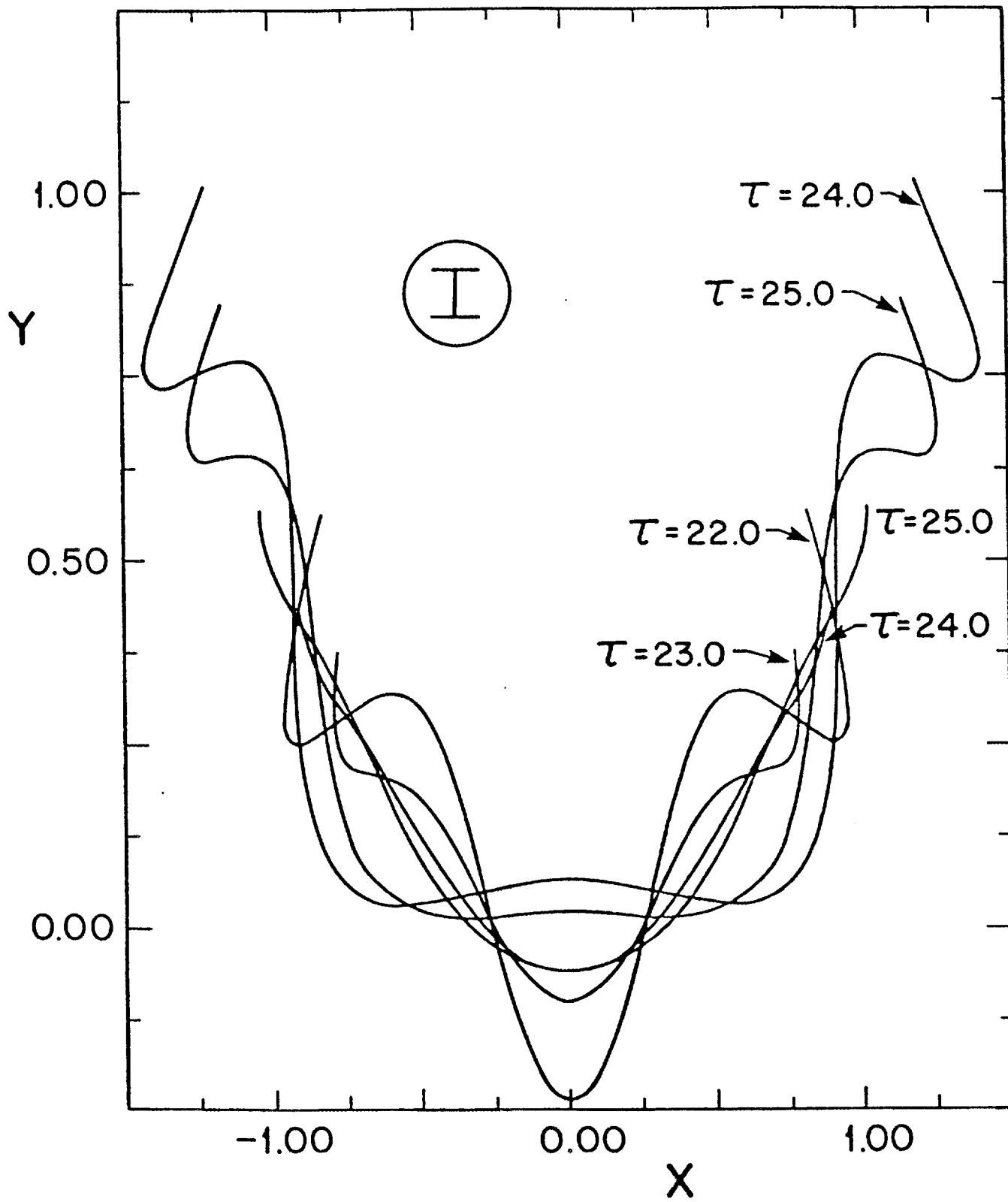


Fig. 16

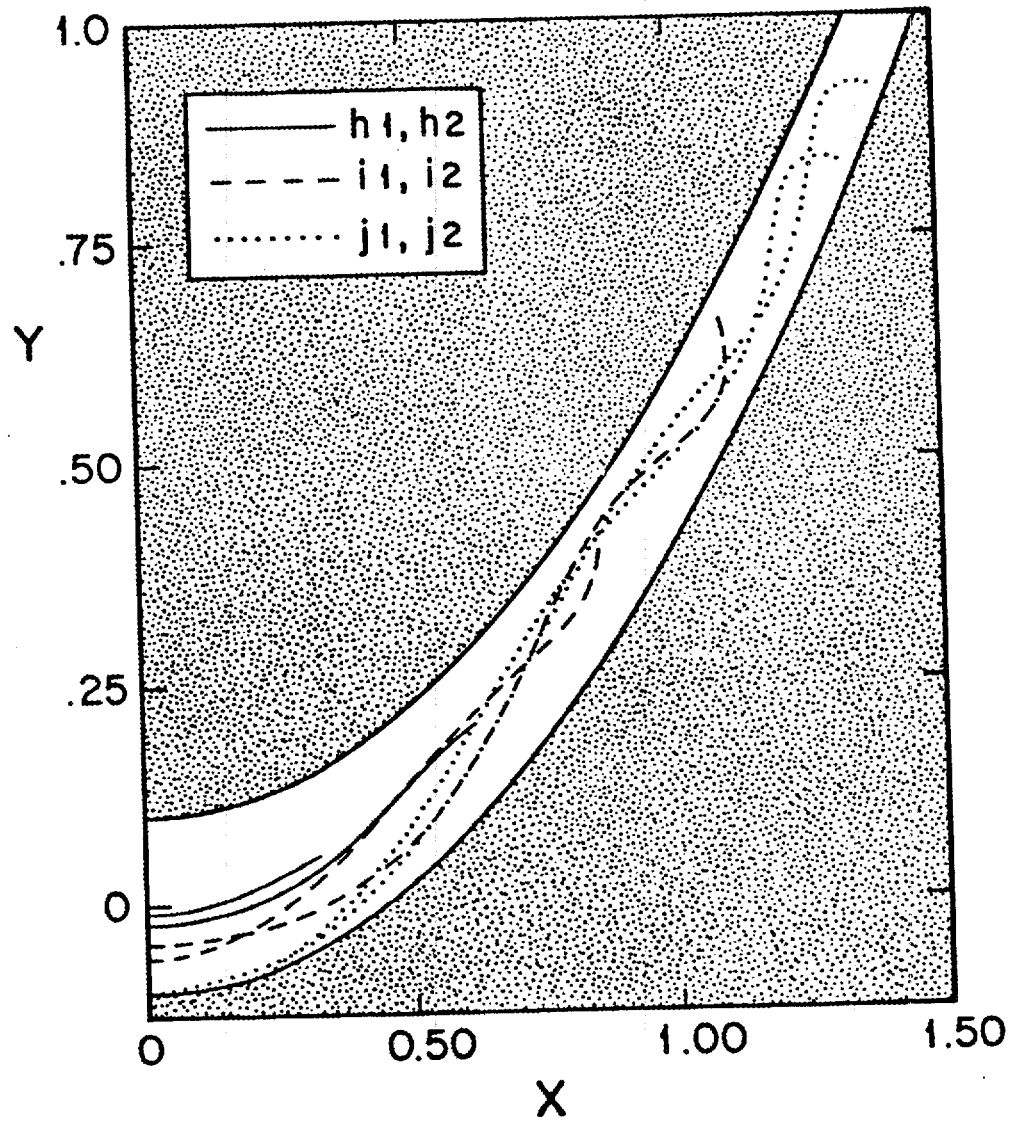


Fig. 17

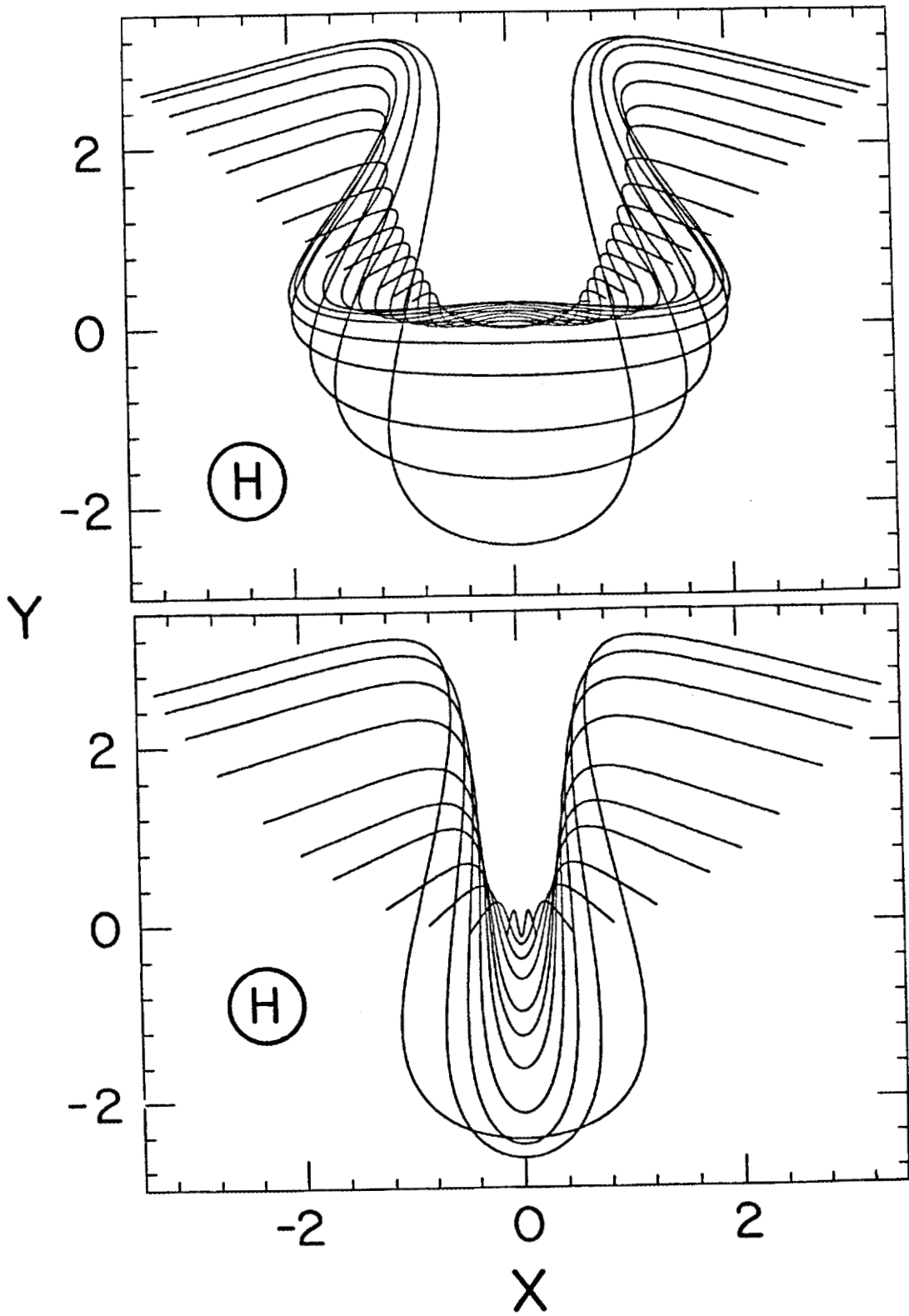
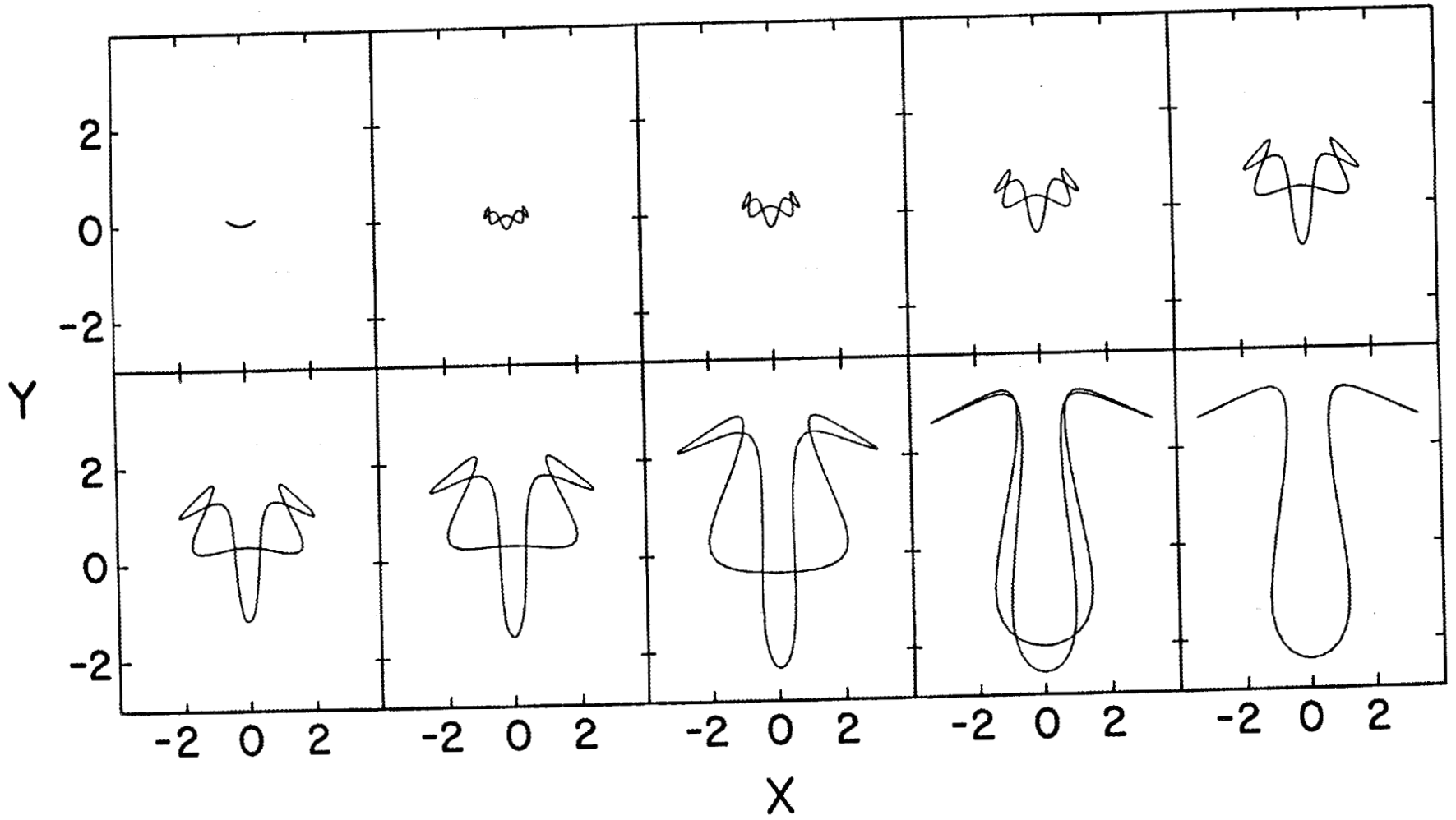


Fig. 18

Fig. 19



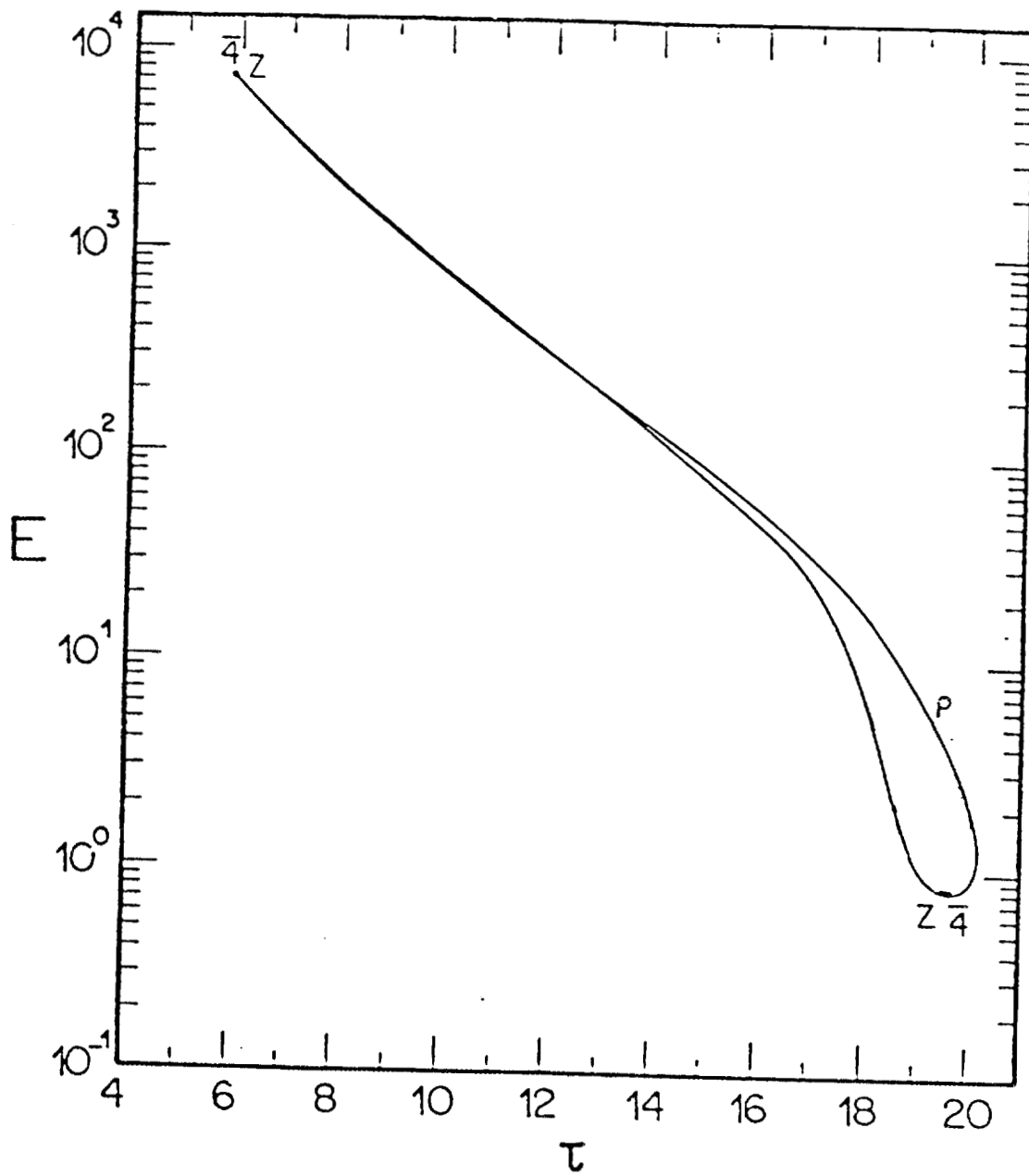


Fig. 20



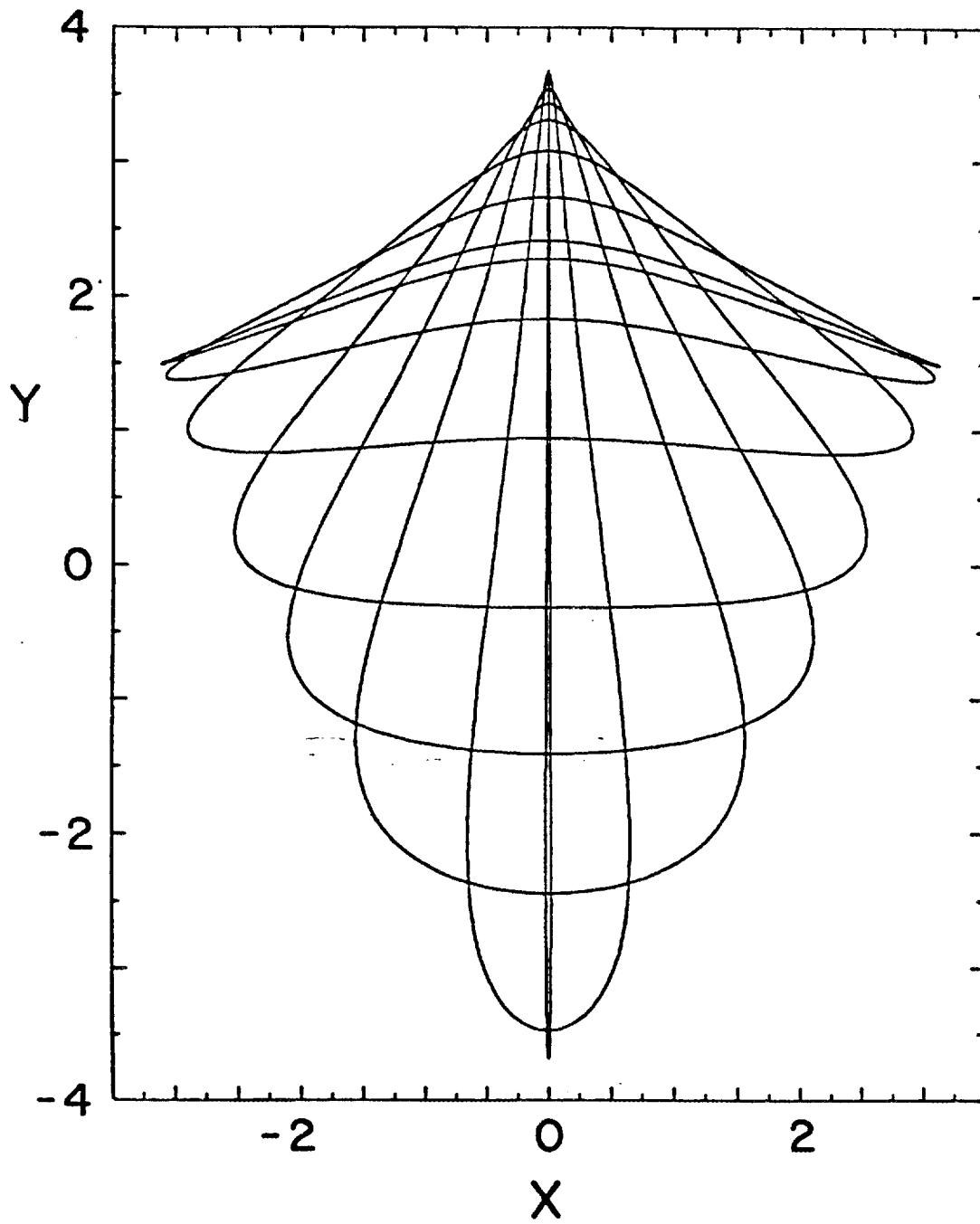


Fig. 22

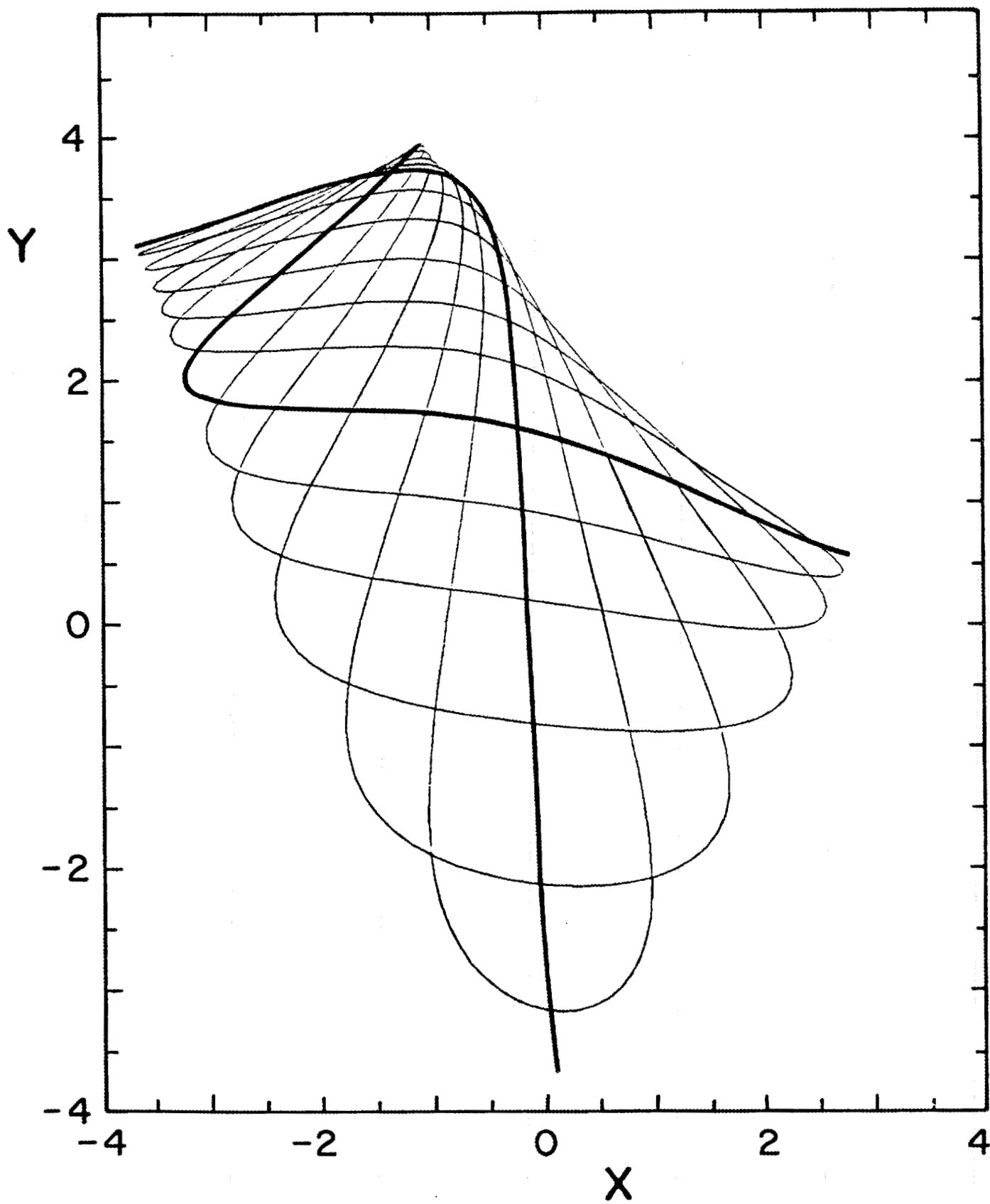


Fig. 23

Fig. 24

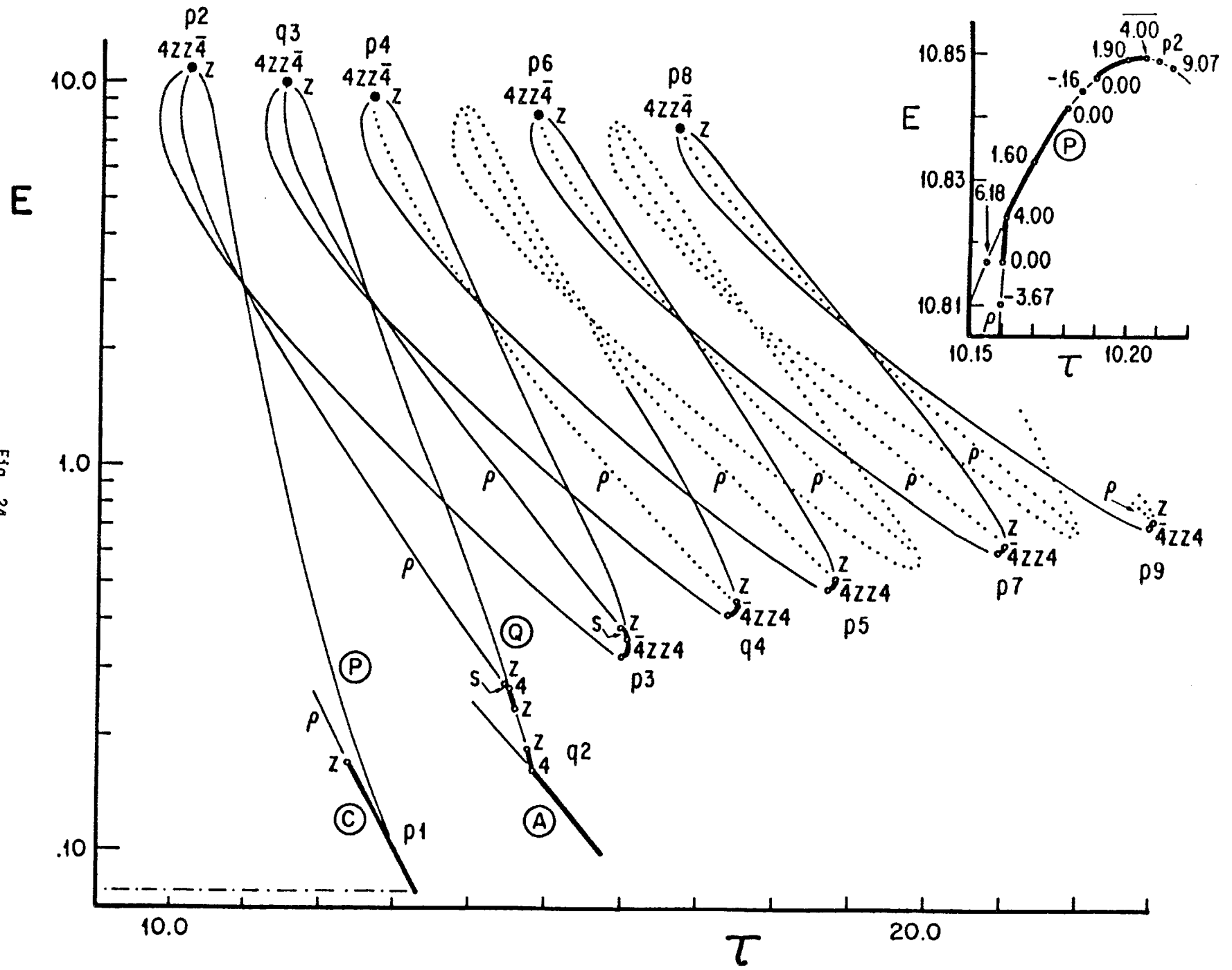
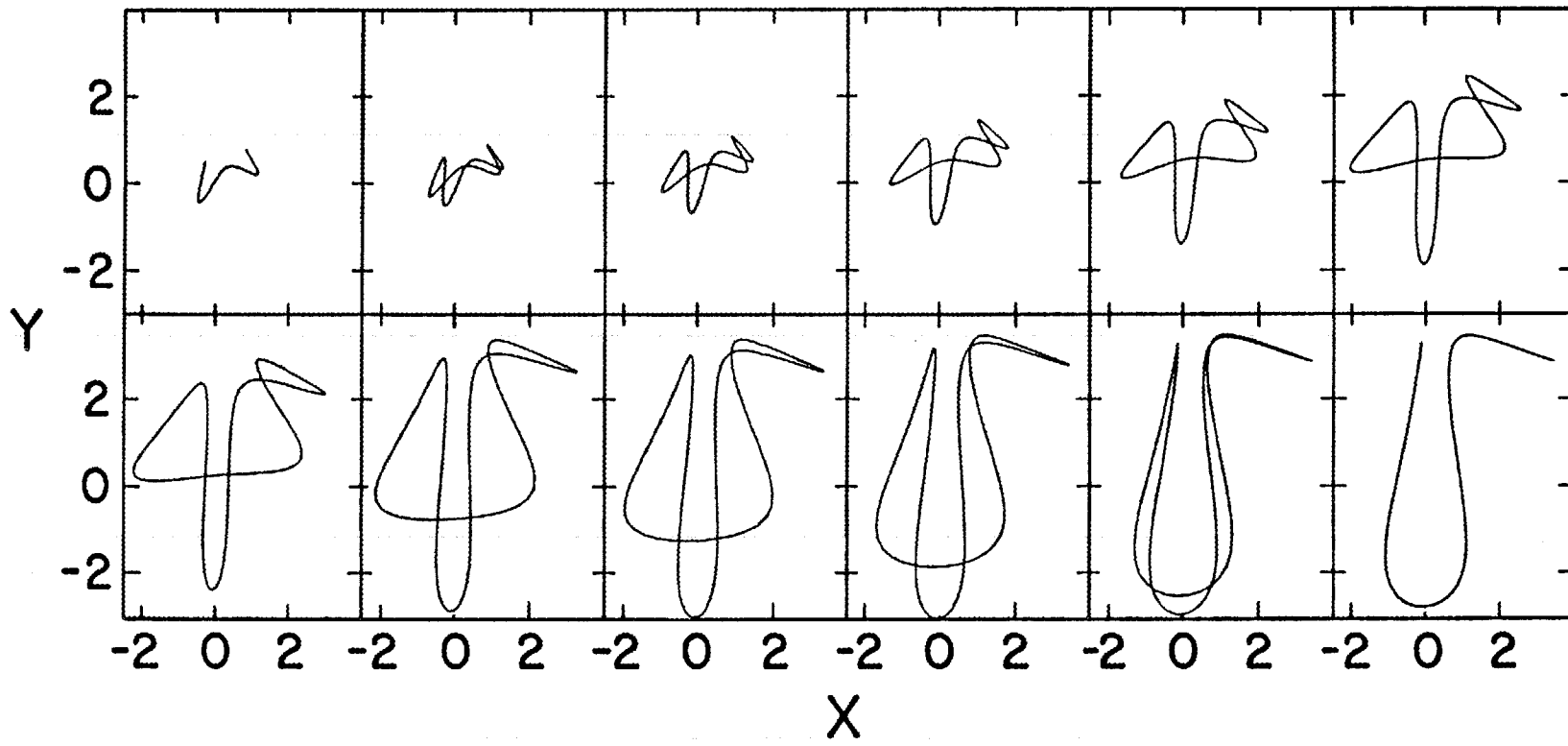


Fig. 25



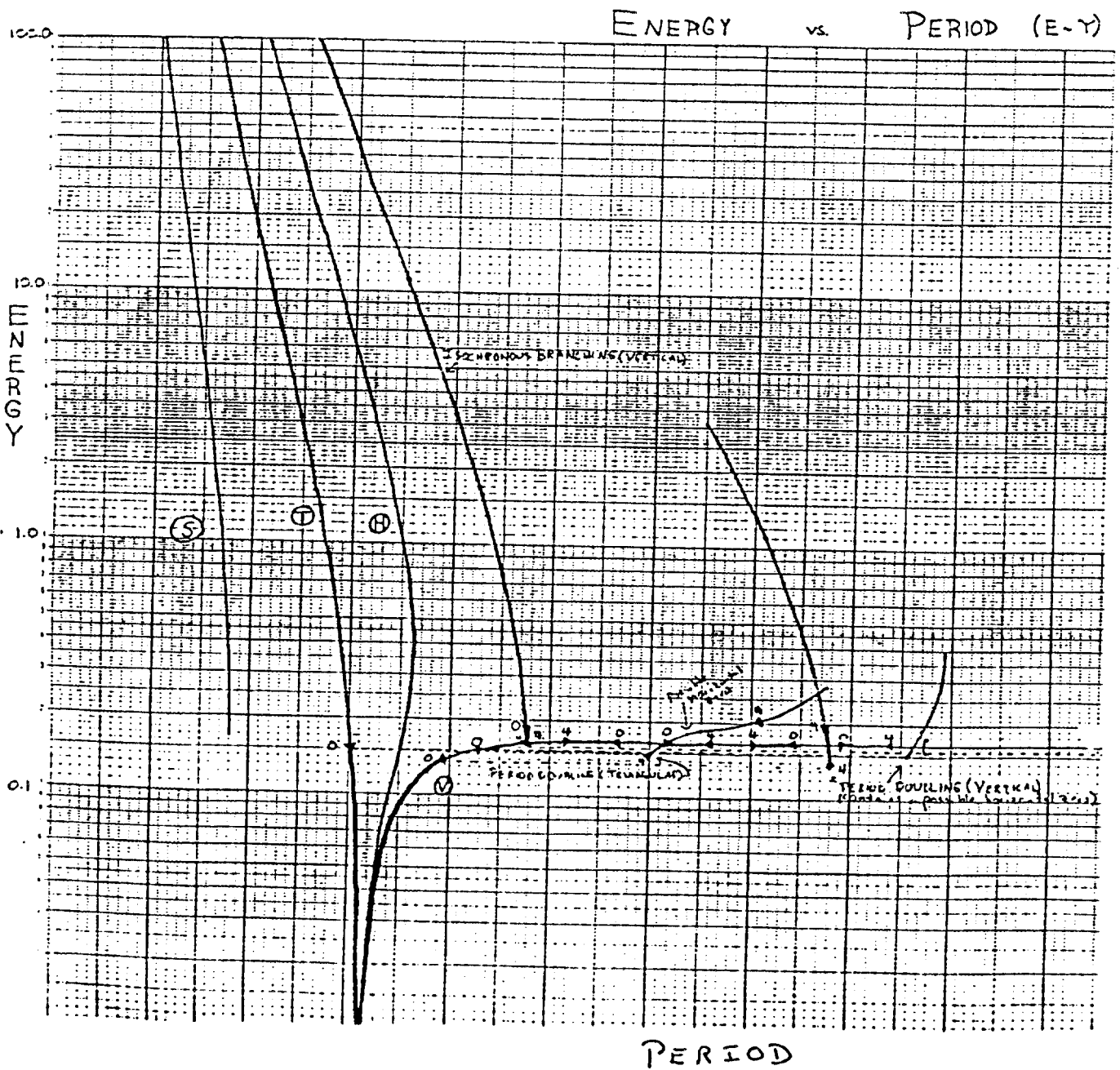


Fig. 26

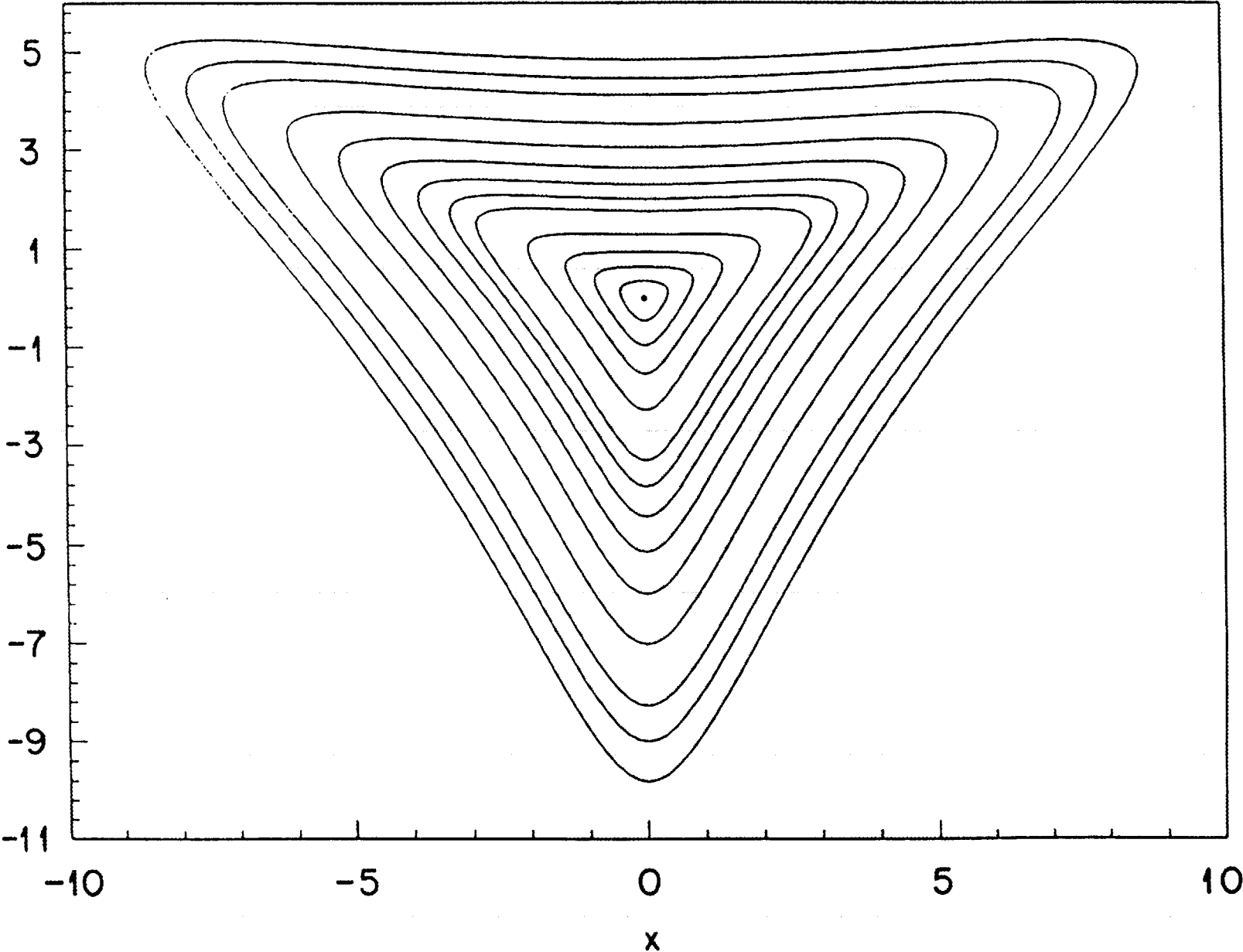


Fig. 27

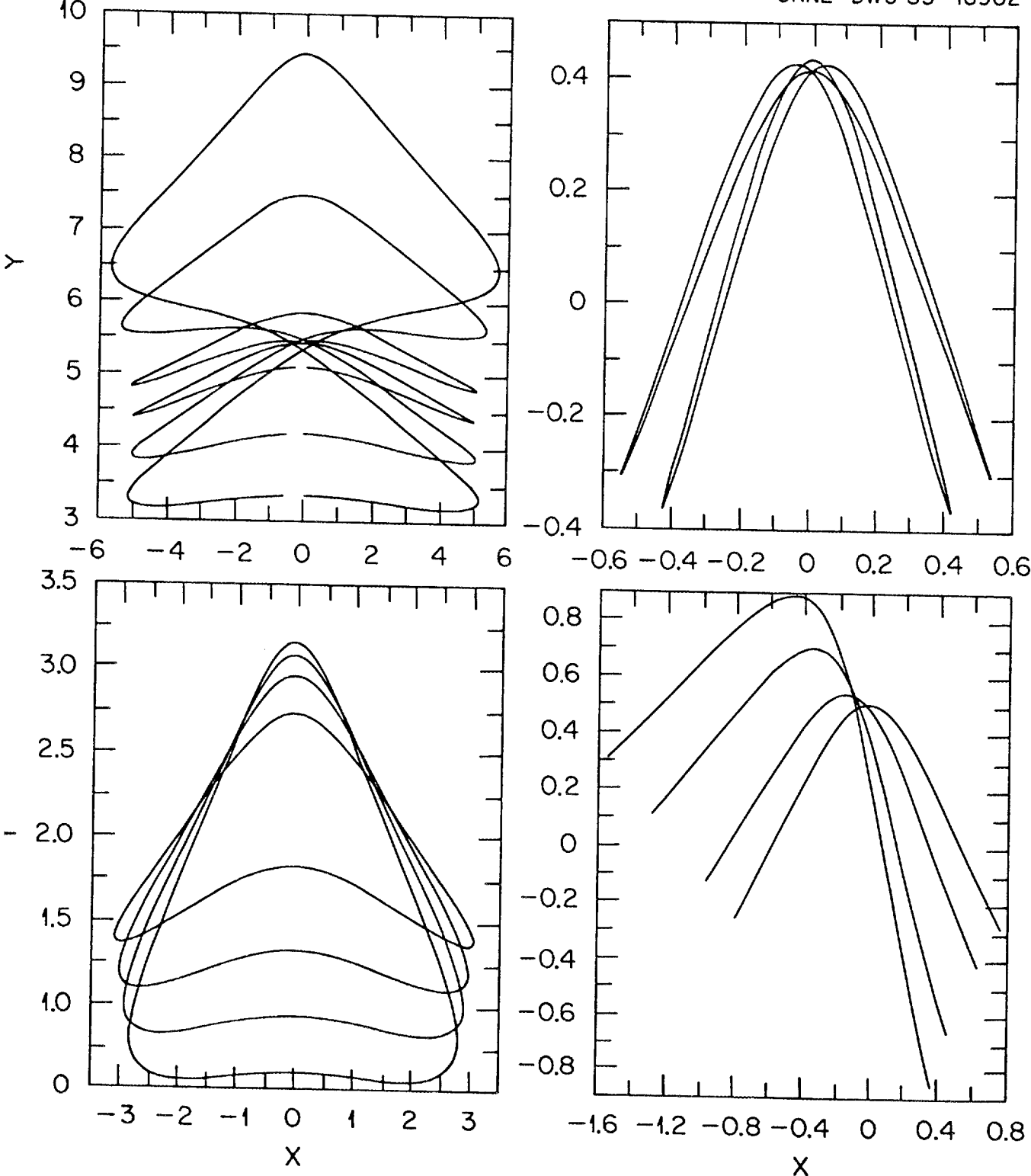


Fig. 28

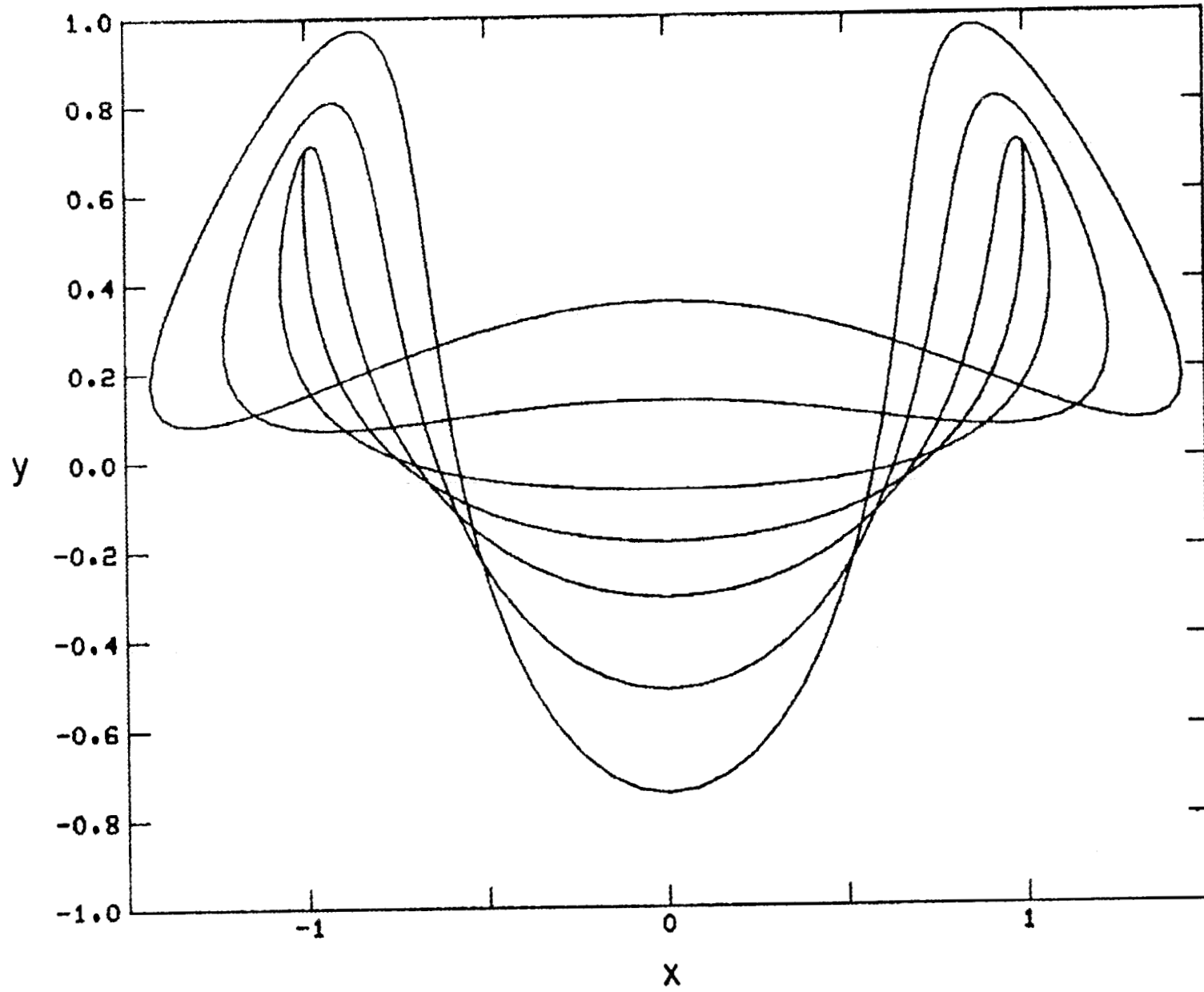


Fig. 29

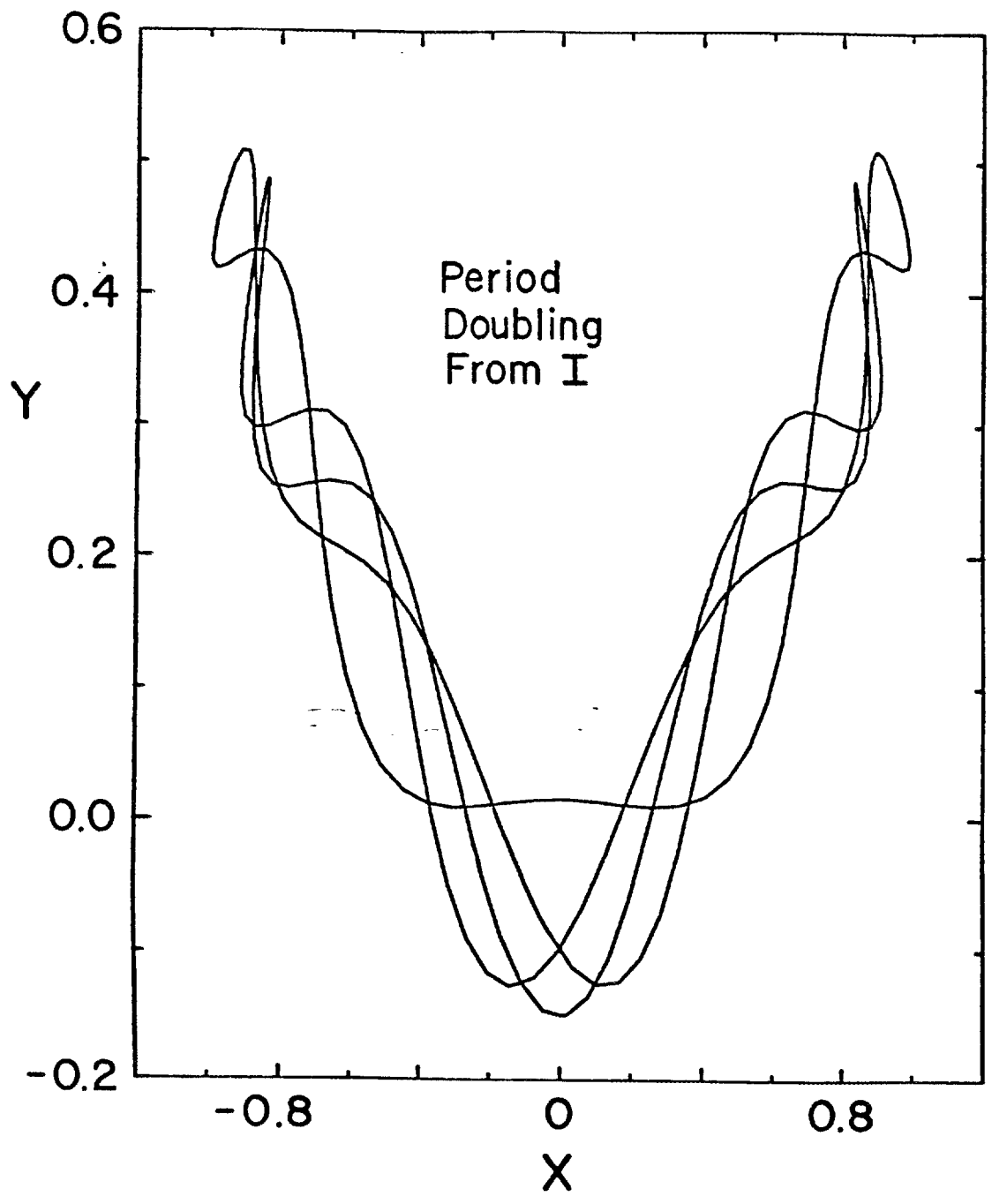


Fig. 30

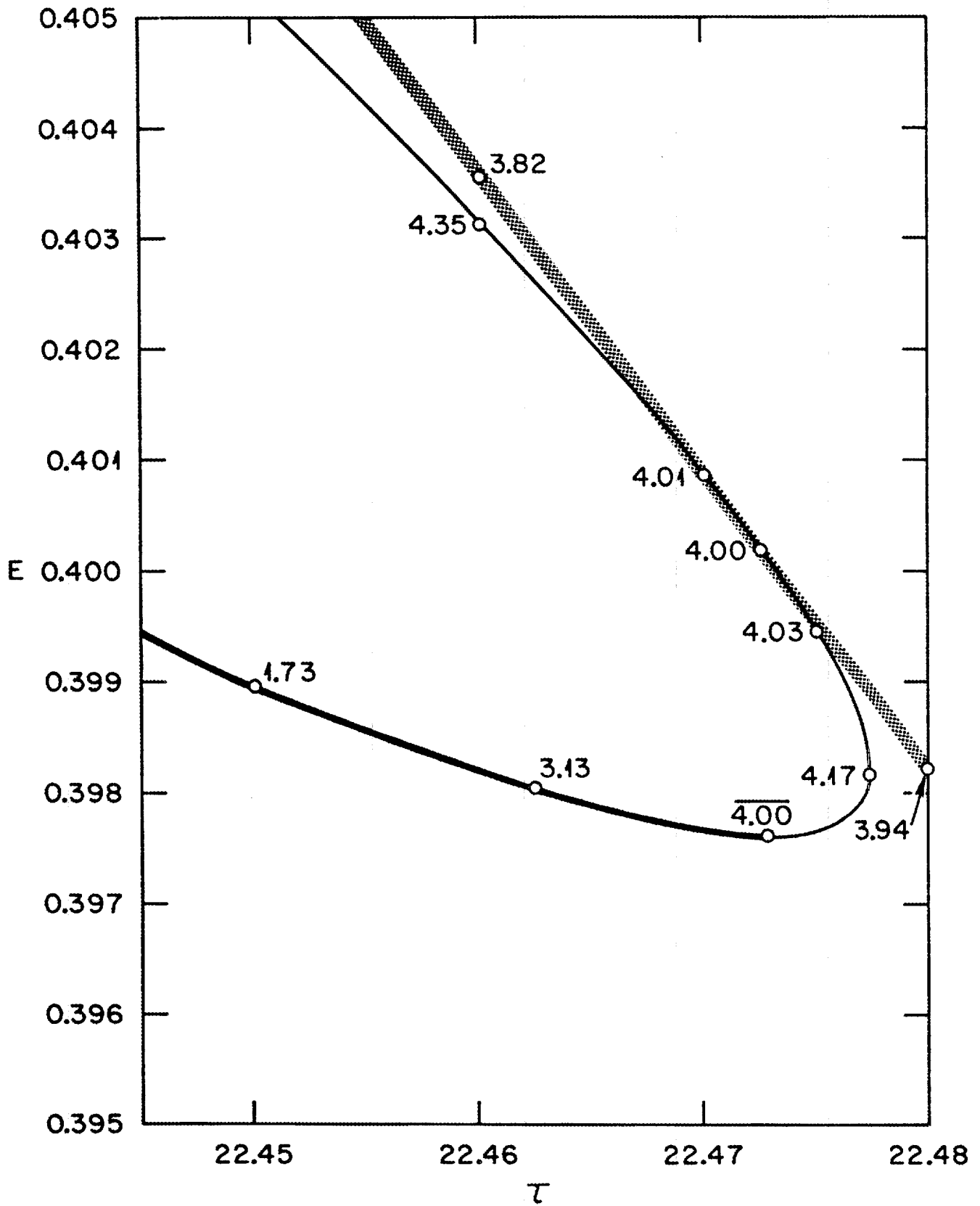
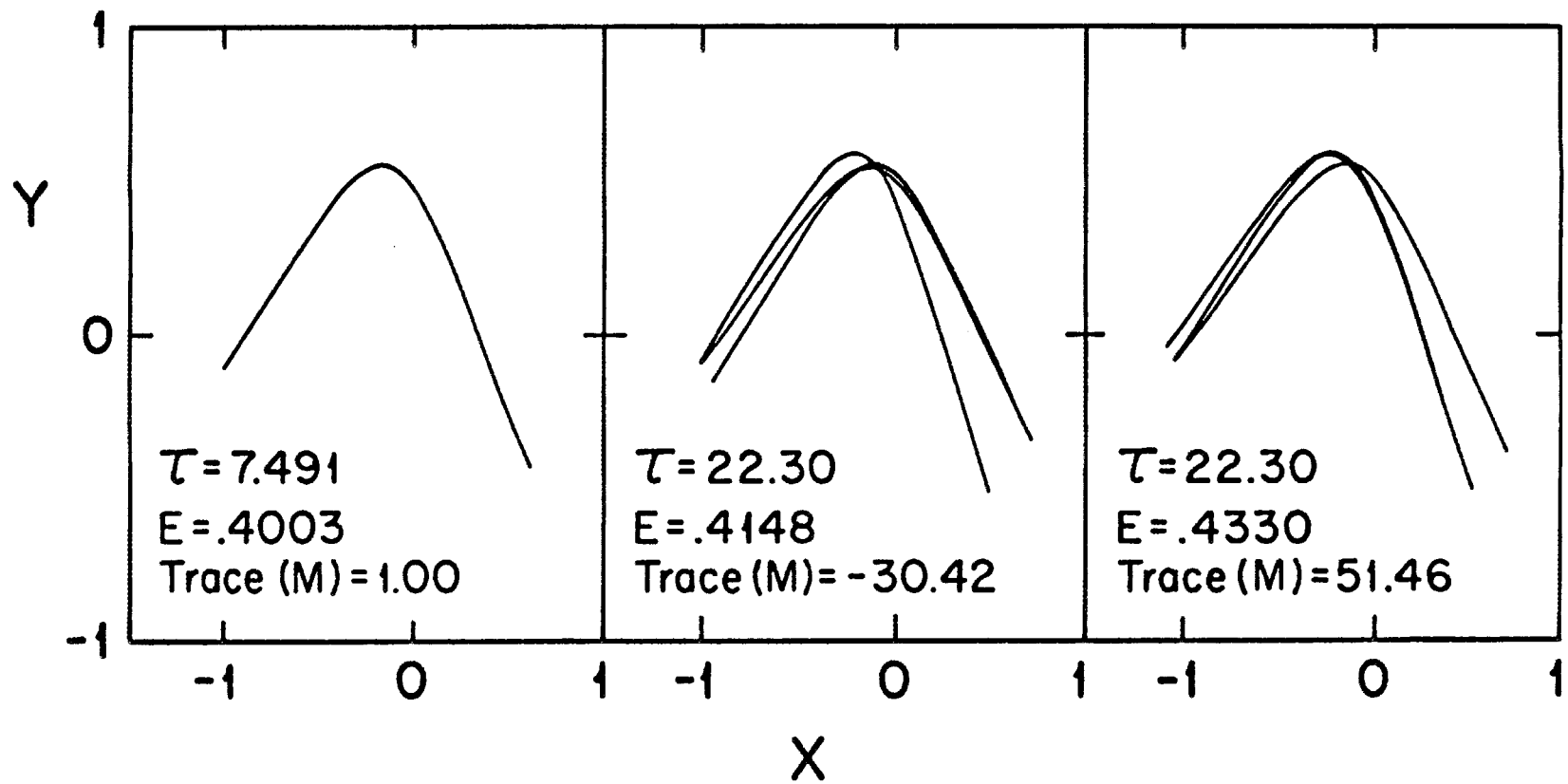


Fig. 31

Fig. 32



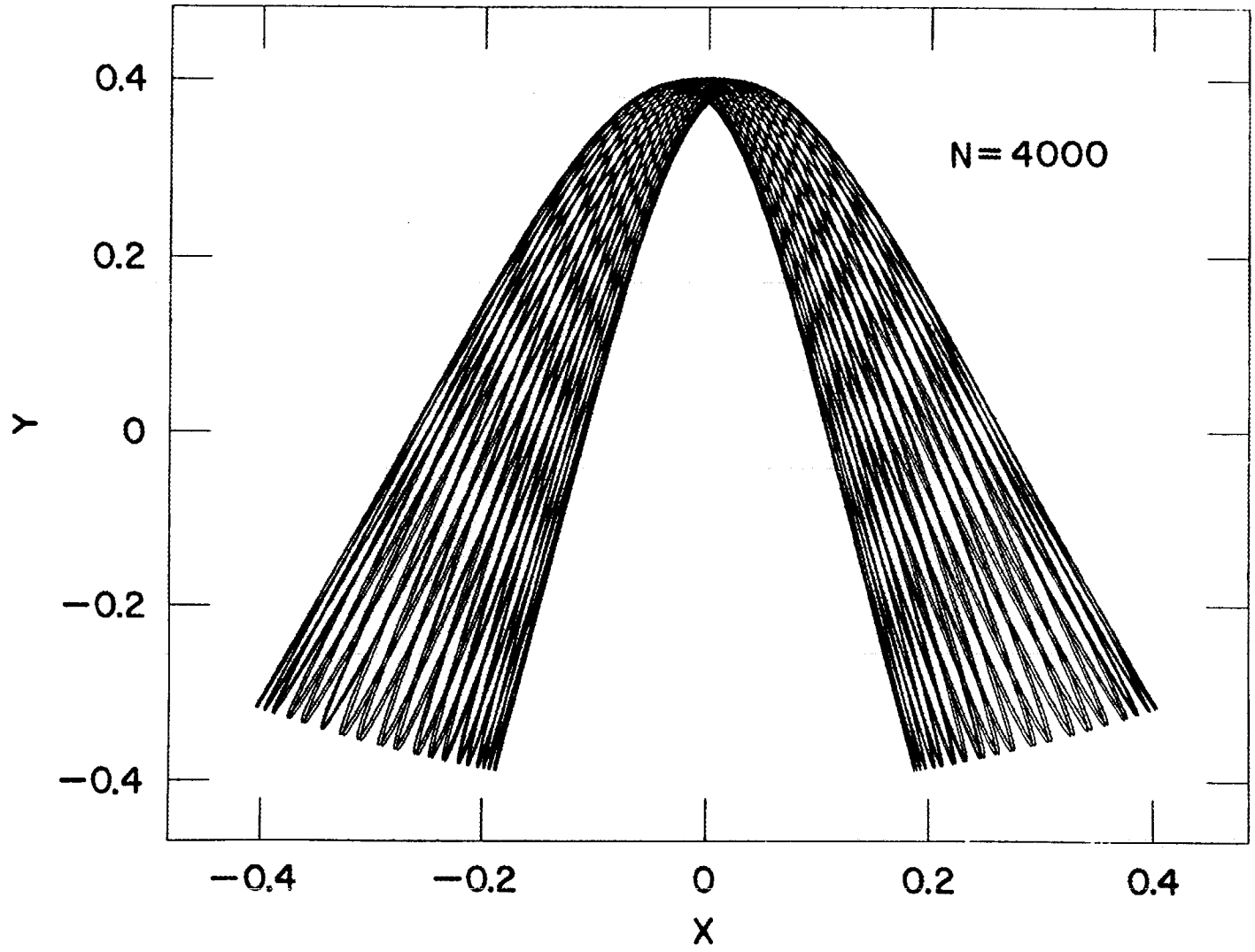


Fig. 33

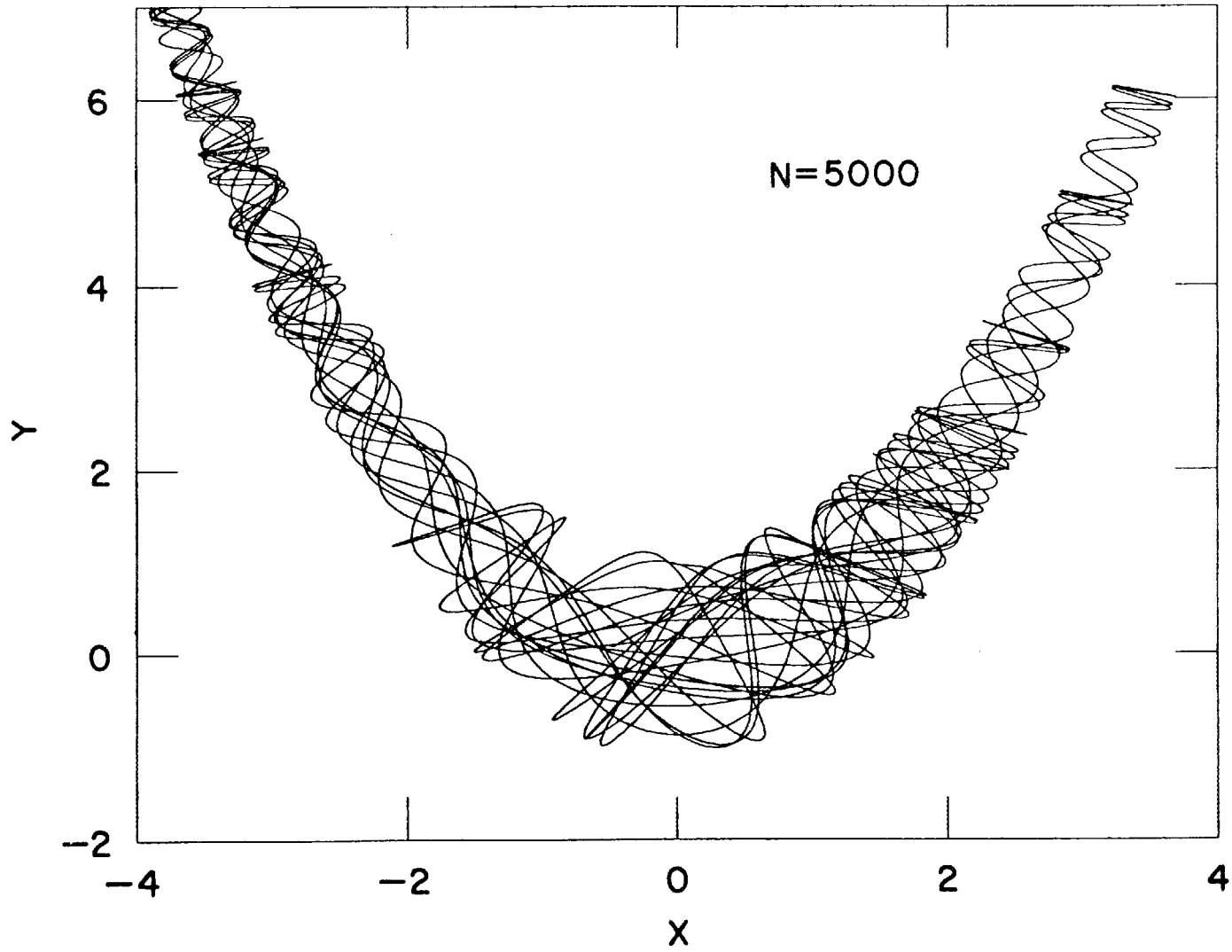
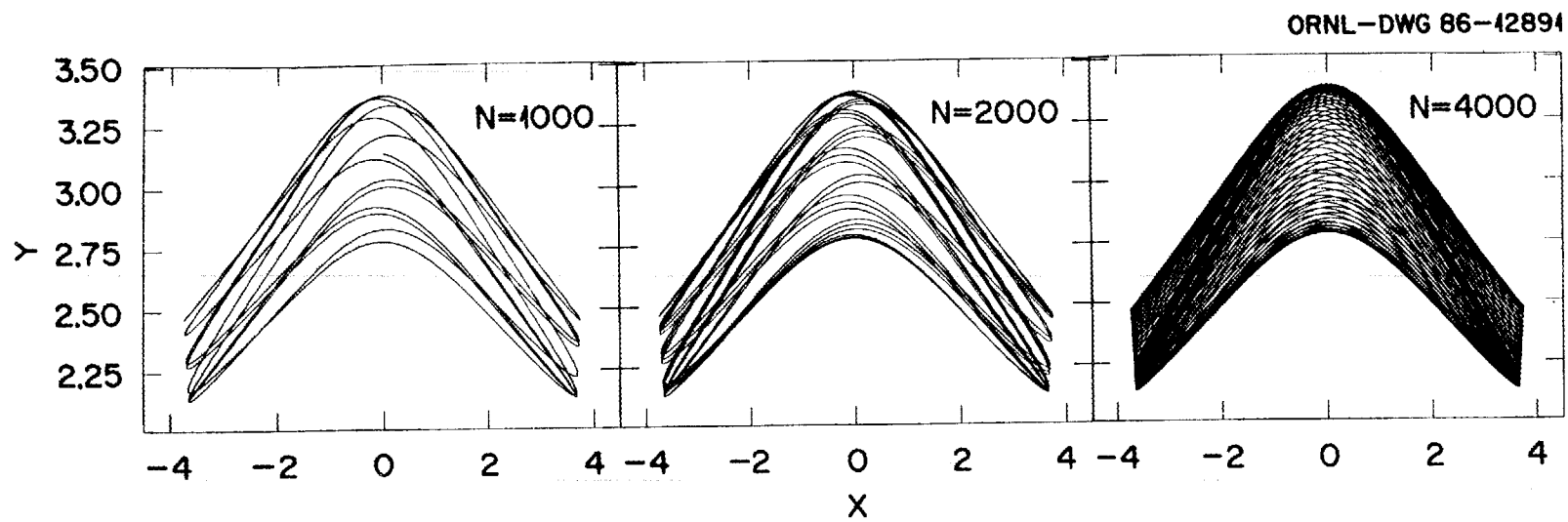


Fig. 34

Fig. 35



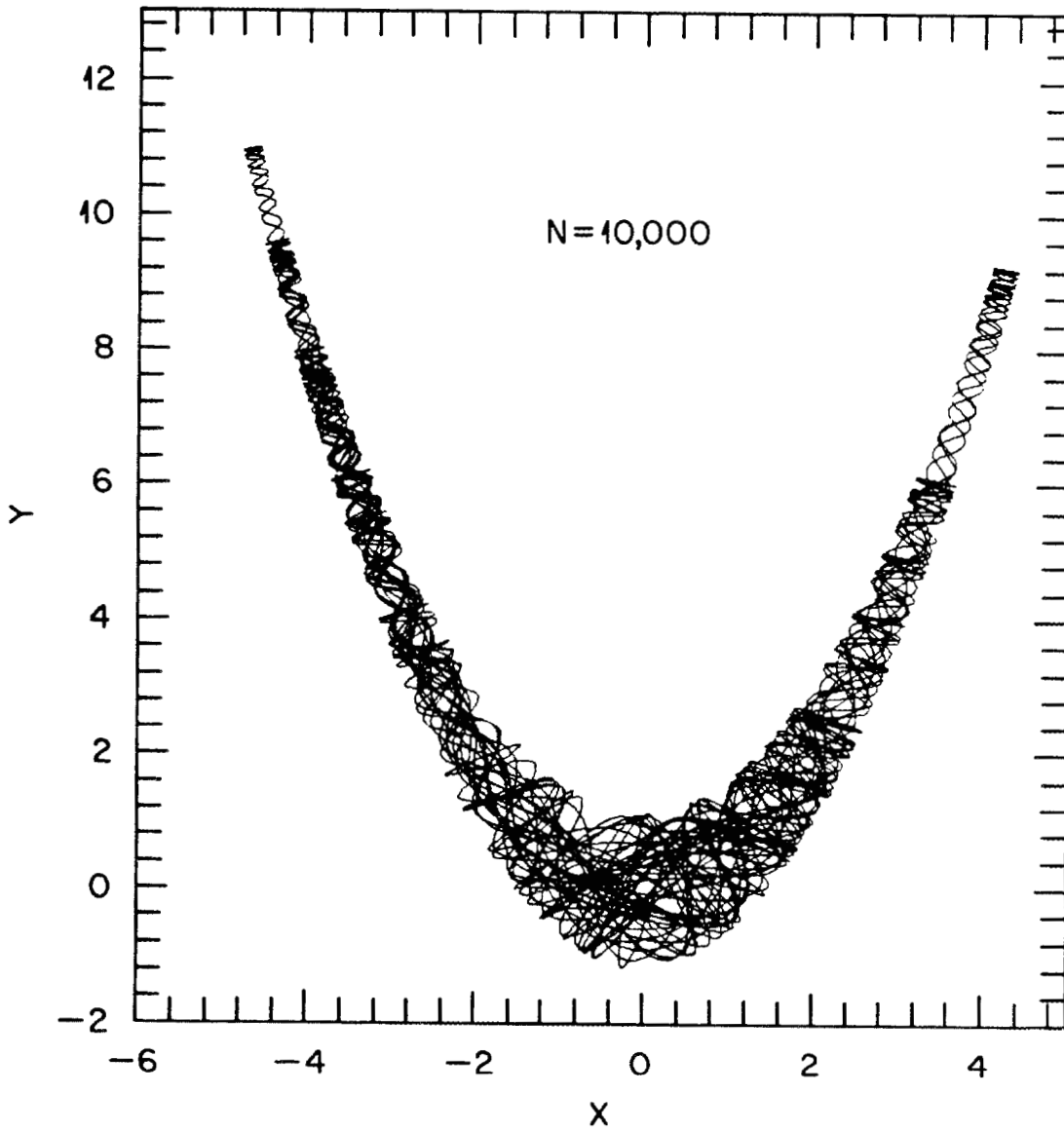


Fig. 36

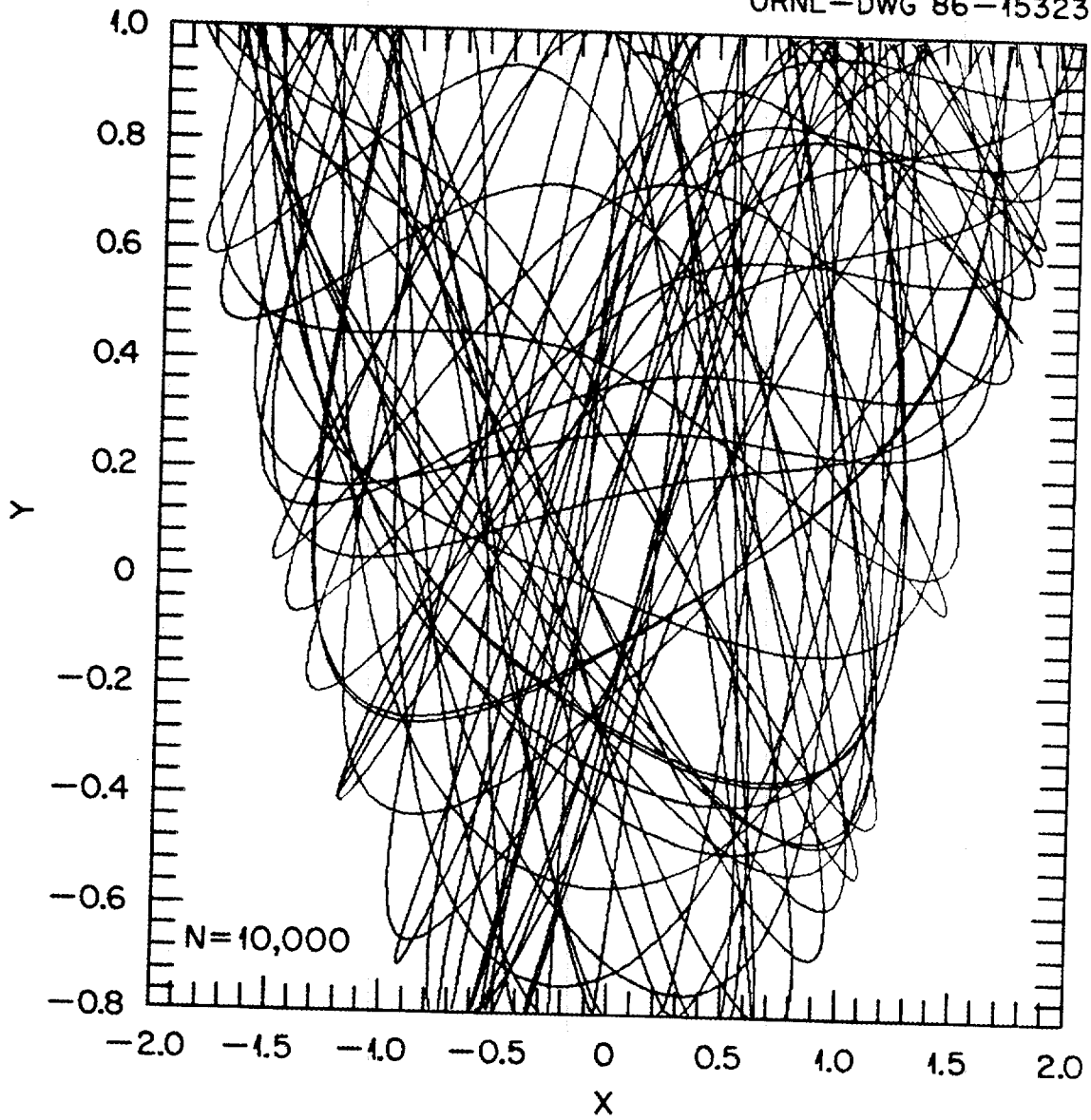


Fig. 37

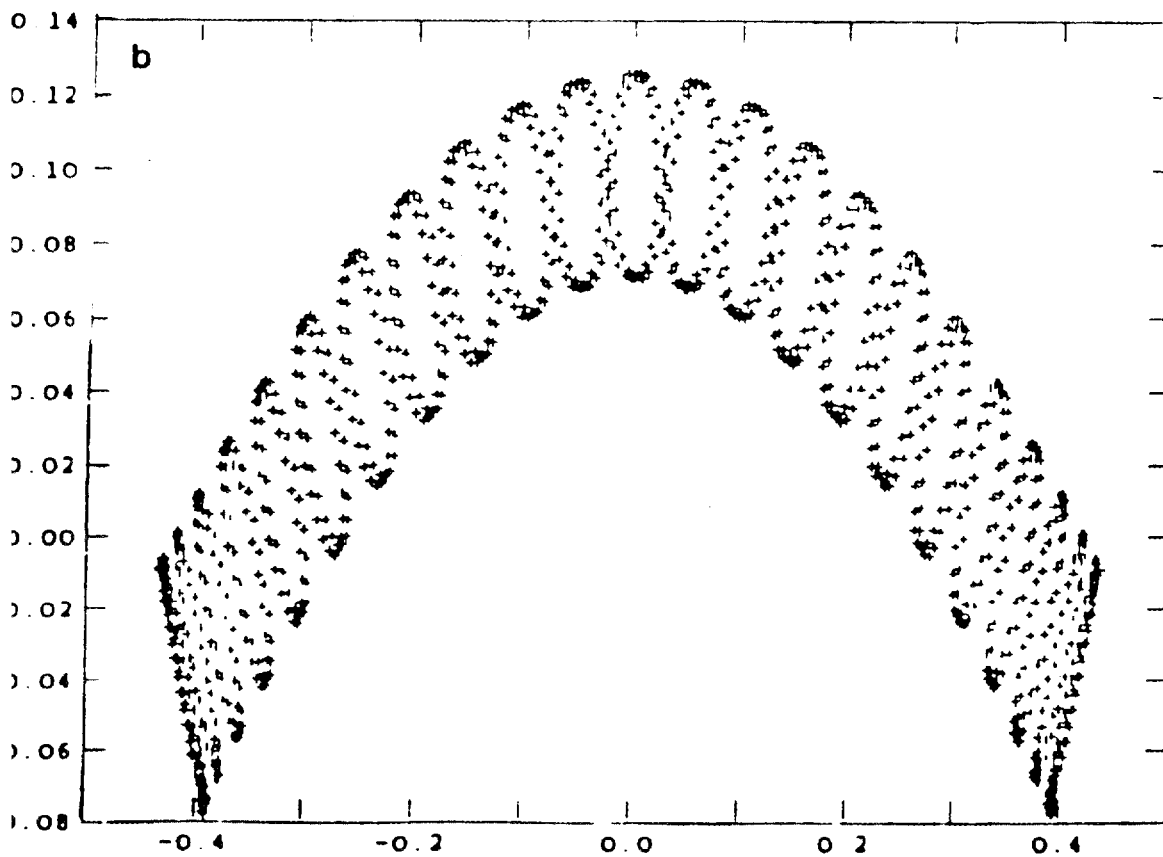
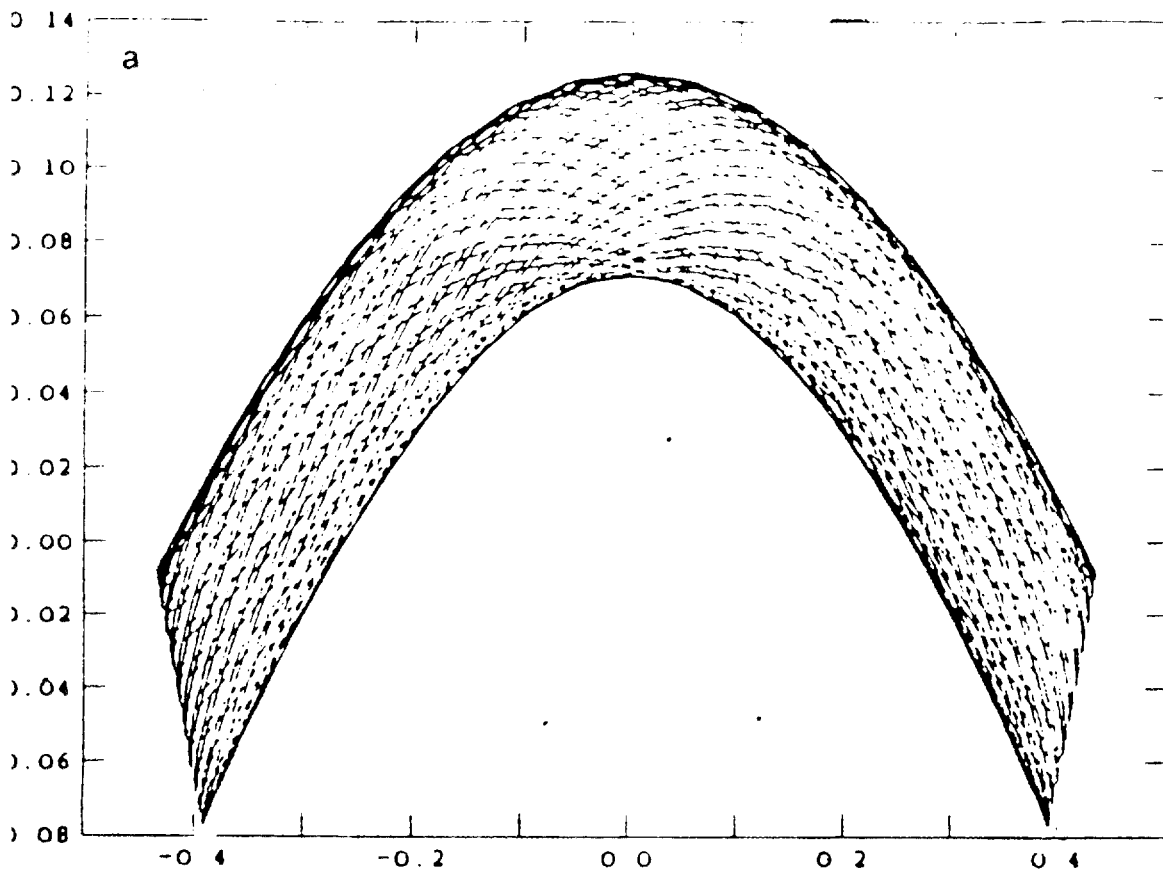
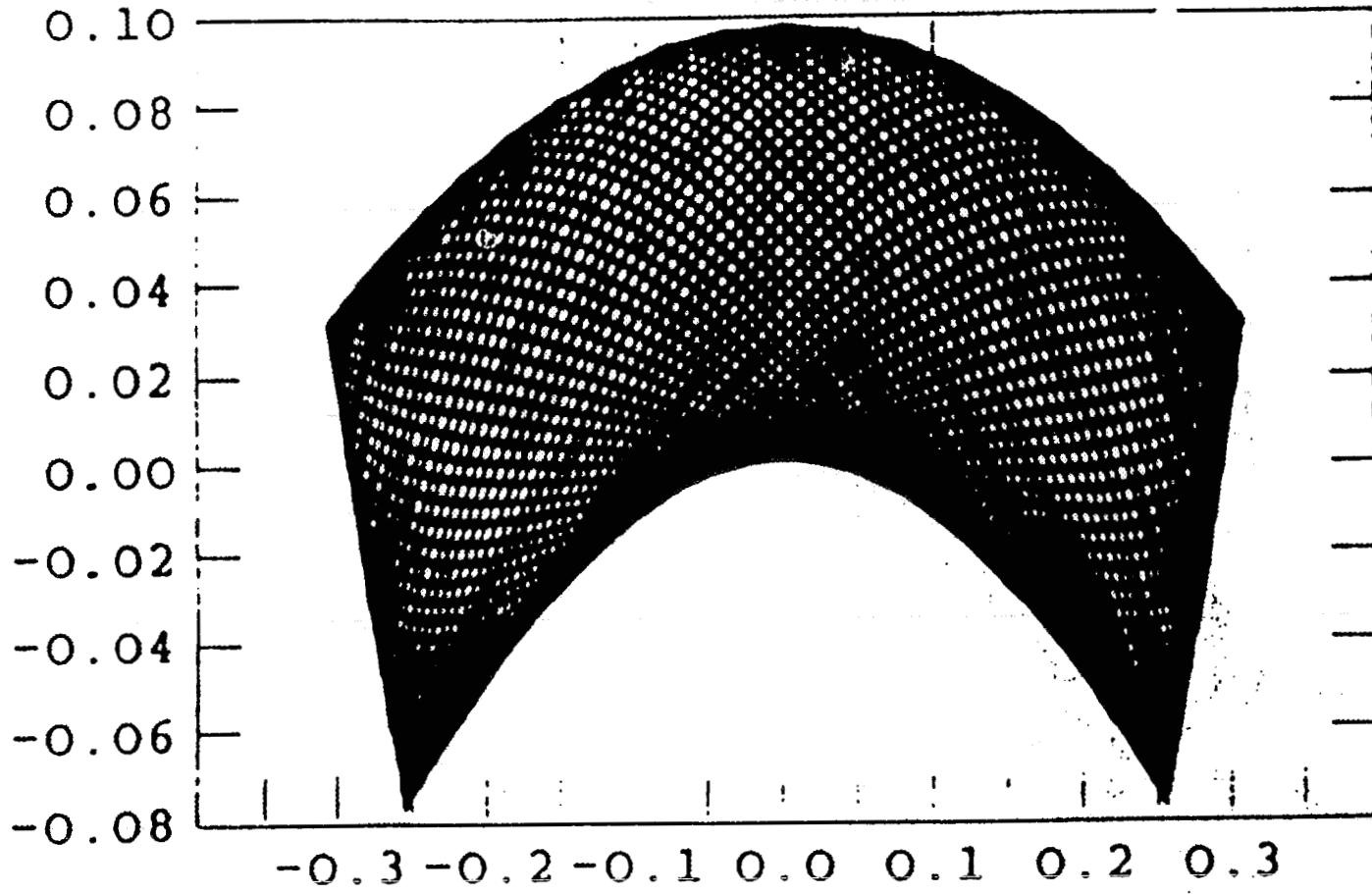


Fig. 38

Fig. 39



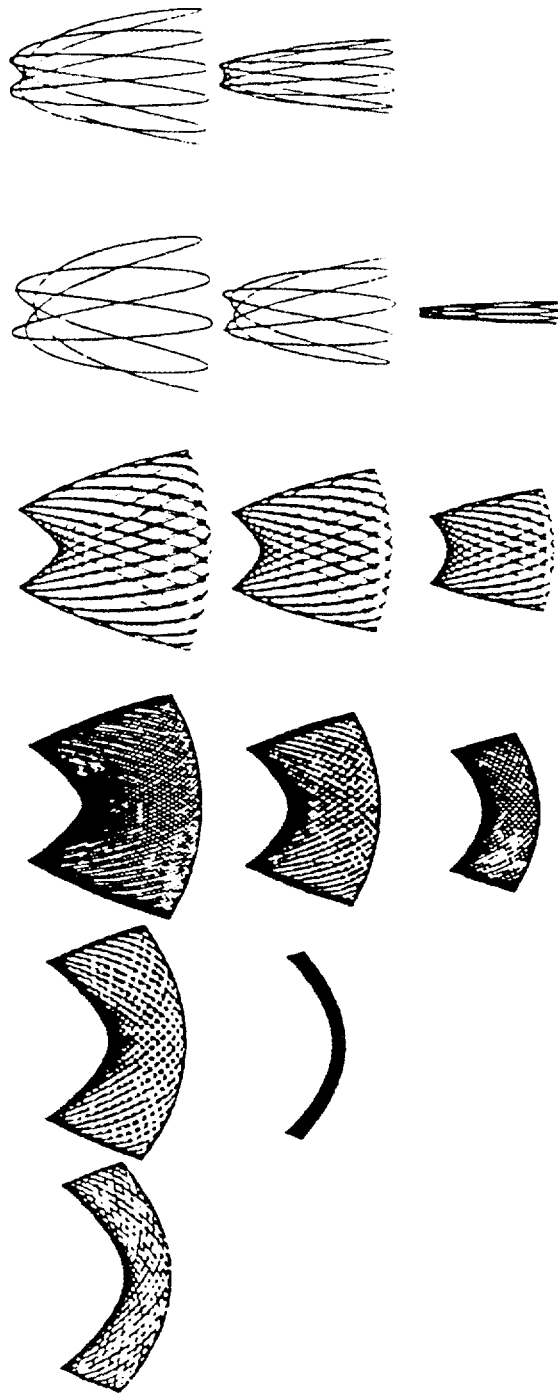


Fig. 40

## INTERNAL DISTRIBUTION

- |                   |                                    |
|-------------------|------------------------------------|
| 1. Y. A. Akovali  | 25. J. H. Macek                    |
| 2. B. R. Appleton | 26. M. J. Martin                   |
| 3. C. Baktash     | 27. J. B. McGrory                  |
| 4. J. B. Ball     | 28. D. W. Noid                     |
| 5. F. E. Barnes   | 29. F. E. Obenshain                |
| 6. R. L. Becker   | 30. F. Plasil                      |
| 7. J. R. Beene    | 31. G. R. Satchler                 |
| 8. C. E. Bemis    | 32. D. Shapira                     |
| 9. C. Bottcher    | 33. P. H. Stelson                  |
| 10. J. Burgdörfer | 34. M. R. Strayer                  |
| 11. N. E. Clapp   | 35. R. L. Varner                   |
| 12. C. S. Daw     | 36. R. C. Ward                     |
| 13. D. J. Downing | 37. C. Y. Wong                     |
| 14. J. D. Garrett | 38. R. F. Wood                     |
| 15. E. E. Gross   | 39. J. Wu                          |
| 16. E. C. Halbert | 40. G. R. Young                    |
| 17. M. L. Halbert | 41. A. Zucker                      |
| 18. D. J. Horen   | 42. Central Research Library (2)   |
| 19. J. E. Jones   | 43. Laboratory Records (2)         |
| 20. T. Kaplan     | 44. Laboratory Records, R.C. (1)   |
| 21. H. Kohn       | ORNL-Y-12 Technical Library        |
| 22. W. F. Lawkins | 45. Document Reference Section (1) |
| 23. I. Y. Lee     | 46. ORNL Patent Section (1)        |
| 24. S. H. Liu     |                                    |

## EXTERNAL DISTRIBUTION

47. M. Baranger, Rm. 6-312, M.I.T., Cambridge, Massachusetts 02139
48. P. Carruthers, Department of Physics, University of Arizona, Tucson, Arizona 85721
49. R. Y. Cusson, Science Applications International Corporation, Suite C31, 5150 El Camino Real, Los Altos, California 94022
50. R. W. Davies, GTE Laboratories, Inc., 40 Sylvan Road, Waltham, Massachusetts 02154
51. M. Dworzecka, Department of Physics, George Mason University, Fairfax, Virginia 22030
52. M. Eckhause, Department of Physics, College of William & Mary, Williamsburg, Virginia 23185

53. E. Engels, Jr., Department of Physics, University of Pittsburgh, Pittsburgh, Pennsylvania 15213
54. K. A. Erb, Office of Science & Technology Policy, Executive Office of the President, Washington, DC 20506
55. D. J. Ernst, Department of Physics, Texas A&M University, College Station, Texas 77843
56. H. Feldmeier, G.S.I., Planckstr. 1, Postfach 110552, D-6100 Darmstadt, West Germany
57. D. H. Feng, Department of Physics & Atmospheric Science, Drexel University, Philadelphia, Pennsylvania 19104
58. H. Flocard, Division de Physique Théorique, Institut de Physique Nucléaire, B.P. N° 1, F-91406 Orsay Cedex, France
59. R. T. Folk, Department of Physics, Building 16, Lehigh University, Bethlehem, Pennsylvania 18015
60. J. J. Griffin, Department of Physics, University of Maryland, College Park, Maryland 20742
61. D. R. Harrington, Serin Physics Laboratory, Rutgers University, P. O. Box 849, Piscataway, New Jersey 08854
62. R. M. Haybron, Department of Physics, Cleveland State University, Euclid Avenue, Cleveland, Ohio 44115
63. G. R. Hoy, Department of Physics, Old Dominion University, Norfolk, Virginia 23529
64. M. B. Johnson, LAMPF, Los Alamos National Laboratory, Los Alamos, New Mexico 87545
65. H. Killory, Department of Physics, University of Akron, Akron, Ohio 44325
66. S. E. Koonin, 106-38, California Institute of Technology, Pasadena, California 91125
67. C. P. Malta, Instituto de Fisica, Universidade de São Paulo, C.P. 20516, 01498 São Paulo, SP, Brazil
68. M. H. Macfarlane, Department of Physics, Indiana University, Bloomington, Indiana 47405
69. J. A. Maruhn, Institut für Theoretische Physik, Universität Frankfurt/M., Robert-Mayer-Strasse 8-10, 6 Frankfurt/M. 1, West Germany

70. R. J. McCarthy, Kent State University, West 9th Street, Ashtabula, Ohio 44004
71. B. Müller, Department of Physics, Duke University, Durham, North Carolina 27706
72. J. W. Negele, 6-308, M.I.T., Cambridge, Massachusetts 02139
73. J. R. Nix, Nuclear Theory, T-9, MS B279, Los Alamos National Laboratory, Los Alamos, New Mexico 87545
74. P.-G. Reinhard, Institut für Theoretische Physik, Universität Erlangen, Glückstrasse 6, D-8520 Erlangen, West Germany
75. M. J. Rhoades-Brown, Physics Division, Building 1005, Brookhaven National Laboratory, Upton, New York 11973
76. E. Rost, Department of Physics, University of Colorado, Boulder, Colorado 80302
77. F. Sakata, Institute for Nuclear Study, University of Tokyo, Tanashi, Tokyo 188, Japan
78. P. B. Shaw, Department of Physics, Pennsylvania State University, University Park, Pennsylvania 16802
79. P. J. Siemens, Department of Physics, Oregon State University, Corvallis, Oregon 97331
80. A. J. Sierk, T9, MS B 279, Los Alamos National Laboratory, Los Alamos, New Mexico 87545
81. R. A. Sorensen, Department of Physics, Carnegie-Mellon University, Pittsburgh, Pennsylvania 15213
82. M. Soyeur, Laboratoire National Saturne, C.E.N. Saclay, F 91191 Gif-sur-Yvette Cedex, France
83. F. Tabakin, Department of Physics & Astronomy, University of Pittsburgh, Pittsburgh, Pennsylvania 15260
84. A. S. Umar, Department of Physics & Astronomy, Vanderbilt University, Nashville, Tennessee 37235
85. J. P. Vary, Department of Physics, Iowa State University, Ames, Iowa 50011
86. D. Vautherin, Division de Physique Théorique, Institut de Physique Nucléaire, B.P. N° 1, F-91406 Orsay Cedex, France
87. G. D. White, Department of Physics, Northwestern State University, Natchitoches, Louisiana 71457

88. Office of Assistant Manager for Energy Research and Development, Department of Energy, Oak Ridge Operations Office, Oak Ridge, Tennessee 37831
- 89-98. Office of Scientific and Technology Information, Department of Energy, Oak Ridge Operations Office, Oak Ridge, Tennessee 37831